EPHYL
IoT waveforms

PROJET FINANCÉ PAR L'ANR - PROJECT FUNDED BY THE ANR
ANR

Enhanced PHY for Cellular Low power communication IoT

D3.1: First results on RRM enablers for massive and dense IoT access

Authors:
ISEP: Lina Mroueh (*Editor*), Yi Yu
Centrale-Supelec: Marwa Chafi, Carlos Bader
INRIA: Diane Duchemin, Jean-Marie Gorce
CEA-Leti: Francois Dehmas
Sequans: Guillaume Vivier

Revision: 1.0

Nov. 2017

SEQUANS COMMUNICATIONS
cea
isep École d'ingénieurs du numérique
Inria INVENTEURS DU MONDE NUMÉRIQUE
CentraleSupélec

Executive Summary

This report studies different aspects of Radio Resource Management in a Narrow-Band (NB-IoT) network. Different uplink design challenges are addressed including the optimization of the spectral efficiency, the extension of the coverage, the reduction of the energy consumption, the improvement of the reliability, and the minimization of the latency. The first part of this report focuses on the tradeoff between the energy consumption of sensor nodes, the allocated bandwidth and the coverage. The average behavior of the network is considered by assuming the sensors and the collectors are distributed according to a random Poisson Point Process that is marked by the channel randomness. Given the collectors density and considering different antennas configurations at the receiver side, a statistical estimation of the size of bandwidth required to handle the overall traffic is provided. The second part of this report presents dynamic spectrum access technique that is derived from machine learning to extend the network coverage while minimizing the number of retransmission and hence the energy consumption. While slotted ALOHA protocol randomly selects the channel to establish connection with the cell, the dynamic spectrum access learns the channel which is more likely to be available and in a normal coverage conditions. The third part of this report presents new techniques based on compressive sensing to improve the network reliability and to minimize its latency.

Notation

BPSK	Binary Phase Shift Keying
BOMP	Block Orthogonal Matching Pursuit
BS	Base Station
CE	Coverage Enhancement
CS	Compressive Sensing
CSI	Channel State Information
FDMA	Frequency Division Multiple Access
GUDSR	Group User Detection Success Rate
IC-NBOMP	Interference Cancellation Normalized Block Orthogonal Matching Pursuit
I-eDRX	Idle mode Extended Discontinuous Reception
IoT	Internet of Things
ISM	Industrial Scientific and Medical band
LASSO	Least Absolute Shrinkage and Selection Operator
LPWAN	Low Power Wide Area Network
LTE	Long Term Evolution
LTE-M	Long Term Evolution Machine Type Communication
MAB	Multi-Armed Bandit
MCL	Maximum Coupling Loss
ML	Maximum Likelohood
MRC	Maximum Ratio Combiner
NB-IoT	Narrow-Band Internet of Things
NBOMP	Normalized Block Orthogonal Matching Pursuit
NOMA	Non Orthognal Multiple Access
OMP	Orthogonal Matching Pursuit
PPP	Poisson Point Process
PSM	Power Saving Mode
PUSCH	Physical Uplink Shared Channel
QPSK	Quadratic Phase Shift Keying

RR	Radio Resource
RRM	Radio Resource Management
SER	Symbol Error Rate
SIMO	Single Input Multiple Output
SINR	Signal to Interference and Noise Ratio
SISO	Single Input Single Output
SNR	Signal to Noise Ratio
TM	Transmission Mode
UCB	Upper Confidence Band
UE	User Equipment
URLLC	Ultra Reliable Low Latency Communications

Contents

1 Introduction and Motivations

Internet of things (IoT) is becoming an increasingly growing topic due to its promise to change different aspects of our world. As recently predicted by Cisco, there will be 50 billions IoT connected devices by 2020, where each cell supports a massive number of devices (more than 50K connections per cell [1]). This rapid penetration of connected devices has the potential to impact the way we live, we work and how we interact with objects. The massive connected world advertised by IoT emerging companies requires a huge transfer of data, devices with long autonomy, as well as an extended coverage and indoor penetration.

In order to meet the requirements of IoT world, the 3GPP has designed a set of solutions dedicated to connected objects. In its recent Release 13 [1], 3GPP has specified cat-M and NB-IoT, two solutions to provide cellular connectivity to low cost, low power objects. In this report, the focus is given on NB-IoT. The main design objectives of NB-IoT are increased coverage, long battery life (between 10 and 15 years), and low user equipment (UE) device complexity. Other technologies have preceded the proposition of NB-IoT such as the LoRaWan standard [2] and the ultra narrow band protocol used by Sigfox [3], which operate in the unlicensed bands (industrial, scientific and medical (ISM) radio bands), however cellular IoT standards which operate in a licensed spectrum band have been worth the wait. In fact, NB-IoT can be deployed in any of the 2G/3G/4G spectrum (from 450 MHz to 3-5 GHz), since it achieves an excellent co-existence and compatibility performance with legacy cellular systems. NB-IoT needs only a small portion of the existing available cellular spectrum to operate without interfering with it. Hence, NB-IoT provides more reliability and more quality of service (QoS) as it operates in regulated spectrum. Moreover, NB-IoT uses existing cellular network infrastructure, which reduces the deployment costs.

One of the main challenges of Radio Resource Management (RRM) in the uplink of the NB-IoT is to optimize the tradeoff between the energy consumption of the objects (referred here as sensors), the allocated bandwidth at the collector and the density of the collectors in the network. The radio dimensioning problem depends critically on the network parameters including the network load, the antenna configuration, and the required Quality of Service (QoS). Given the density of aggregators and the simultaneously active sensors, dimensioning the LPWA network consists to statistically determine the bandwidth required to serve all sensors with a given confidence margin. The event that arises when the collector has no more radio resources to attribute to active sensors will be denoted by *radio resource outage event*. The first part of this report focuses on the statistical dimensioning problem studied considering different antennas configurations of collectors and different transmission modes (TMs). The average statistical behavior of the network is considered: active sensors and collector are randomly distributed in a given area according to a random Poisson Point Process. The randomness of the wireless channel is considered as a mark of the Poisson position and results from stochastic geometry using marked Poisson Point Process as in [4, 5, 6, 7, 8, 9, 10, 11] will be invoked. These tools were investigated in [12, 13, 14, 15] to compute an upper-bound on the resource outage probability in a cellular network considering random Point Poisson Process marked by the random shadowing. Unlike our previous contributions [12, 13, 14, 15] where we considered that the network is noise limited, this study is more general as it takes into account the impact of interference

on the statistical dimensioning.

To achieve the NB-IoT targets in terms of coverage and long-battery life, several techniques have been adopted, including repetitions, power spectral density boosting, single-tone transmission, power saving mode, phase rotated modulations (e.g $\frac{\pi}{2}$-BPSK and $\frac{\pi}{4}$-QPSK) to reduce peak-to-average power ratio in the uplink and so forth. Repeating transmission data and control signals has been selected as a major solution to enhance coverage of NB-IoT systems. However, this leads to reducing the system throughput and thereby a spectral efficiency loss. Another cost of providing deep indoor coverage is lowering the number of supported devices per sector. Hence, the second part of this report is dedicated for new techniques that extend the coverage while reducing the number of retransmissions.

In the context of Ultra Reliable Low Latency Communications (URLLC), critical applications aim at transmitting a valuable message, which must be received and taken into account within a very short delay. URLLC often relates to remote control or vehicular communications or Tactile Internet, which are out of the scope of this study, but some scenario in context of Internet of Things may require low latency and reliability. For example, alarms and reports for emergency or medical surveillance are thus under consideration. Typically, the ITU and 3GPP recommendations for this 5G devices category mention requirements of physical-layer latency (including transmission, propagation, processing and potential repetitions) of 0.5ms and a block error rate not exceeding 10^{-5} (compared to 10^{-2} for current 4G networks). A trade-off between the time/spectral occupancy for ensuring a high reliability and the latency reduction is then required. Furthermore, in the case of massive IoT LPWA communications, the low energy consumption and spectral efficiency requirements also underline the need for a trade-off in the medium access technique of sporadic communications. In other words, achieving simultaneously low latency, low power consumption and reliability is definitely challenging!

The rest of this report is organized as follows. In Section 2, we define the network model based on marked Poisson Point Process. Then, we determine in Section 3 the size of the bandwidth required by the network to handle the overall traffic. Section 4 proposes dynamic spectrum access strategies based on machine learning to extend the coverage while reducing the number of transmission. Section 5 provides compressive sensing techniques to minimize the latency and to improve the network reliability. Finally, Section 6 concludes this report.

2 Dense and massive IoT network model

We consider a sensor network in which a random number of active nodes (sensors and collectors) are uniformly distributed in a given area $\mathcal{A}$. At a given instant, the number of active nodes is distributed according to a Poisson law with a density that depends on the mean inter-arrival rate and the mean time of service. This framework of assumptions defines the spatial Poisson Point Process (PPP) in which the positions of active nodes are uniform knowing that the number of nodes is Poisson distributed. A mathematical background on spatial Poisson Point Process is provided in Appendix A. In this section, we define the LPWA network model using spatial Poisson Point Process (PPP). Then, we study the adequacy between the use cases considered in D2.1. and

this spatial PPP model compared with other processes.

2.1 LPWA network model

The sensors devices are considered to be distributed in a given area $\mathcal{A}$ according to a spatial PPP Φ_s. We assume that a sensor is active n_a times per day, the mean service time is ν^{-1} (s) and the inter-arrival rate is ρ per s and per km^2. The active sensors nodes form then a spatial PPP Φ_a with intensity

$$\lambda_a = \frac{n_a}{24 \times 60 \times 60} \rho \, \nu^{-1}.$$

We also assume that the LPWAN collectors are distributed according to a PPP Φ_b with intensity λ_b. Given the spatial PPP, the average inter-distance between two collectors is then,

$$d_b = \int_0^\infty 2\pi\lambda_b r^2 e^{-\lambda_b \pi r^2} dr = \frac{1}{2\sqrt{\lambda_b}}.$$

The frequency reuse pattern in the network is equal to 1. At a given collector situated at $y_0 \in \Phi_b$, the received power from a sensor $x \in \Phi_a$ is computed as,

$$P_r(y_0, x) = P_t \, \alpha \, |y_0 - x|^{-\beta} \, A_f A_s$$

where α and β are respectively the attenuation factor and the path-loss exponent that are computed from the Okumura-Hata model, A_f is the fading coefficient with distribution depending on the antenna configuration and A_s the shadowing coefficient with log-normal distribution. The sensor nodes are considered as static and the fading

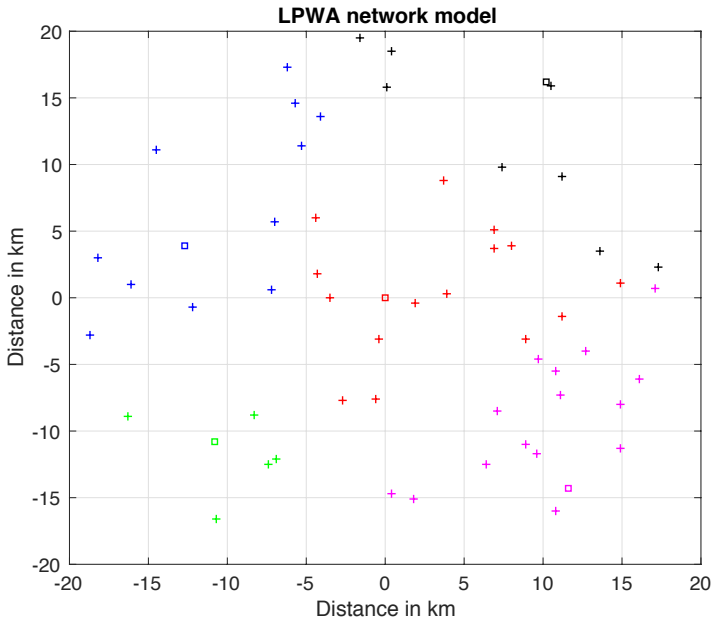

Figure 1: LPWA network model: each sensor is connected to the closest collector on which the average received power is the best. The sensors nodes are illustrated by + and the collectors by a square. The typical cluster contains the red nodes.

channel is considered as flat during the transmission. The Channel State Information (CSI) is only available at the receiver side and not at the transmitter side. Each sensor is connected to the collector on which the average received power (by averaging over the fading and the shadowing) is the highest. This is equivalent to connect the sensor to the nearest collector as illustrated in Figure 1. Assuming a collector y_0, the set of the sensors connected to this latter is defined as:

$$\Phi_c(y_0) = \{x \in \Phi : \forall y \in \Phi_b - \{y_0\} : |y_0 - x| < |y - x|\}.$$

The power of the additive thermal noise is $N_0 = KTB$ with $K = 1.379 \times 10^{-23}$ (W Hz^{-1} K^{-1}), $T = 290$ K and B is the bandwidth. Nodes transmitting in the same frequency band generate additive interference with power

$$I(y_0) = \sum_{x_i \in \Phi_I} P_t \; \alpha \; |y_0 - x_i|^{-\beta} \; A_{f,i} A_{s,i},$$

with

$$\Phi_i = \bigcup_{y \in \Phi_b | \{y_0\}} \{x_i : x_i \text{ randomly selected in } \Phi_c(y)\}.$$

The received SINR at the given collector y_0 is,

$$\text{SINR}(y_0, x) = \frac{P_t \; \alpha \; |y_0 - x|^{-\beta} \; A_f}{N + I(y_0)}$$

with N being the random noise with mean power of N_0 and random additive interference power $I(y_0)$. The power of the random Gaussian noise is characterized by its Laplacian in [5] given by

$$\mathcal{L}_N(s) = \mathbb{E}[e^{-sN}] = \frac{1}{sN_0 + 1}.$$

The Laplacian of the interference field as well as the average size of the network will be further detailed in Subsection 2.1.2 and 2.1.1.

2.1.1 Statistical interference model

Let Φ_I be the set of the interfering nodes that transmit on the same radio resource (RR) such that,

$$\Phi_i = \cup_{y \in \Phi_b | \{y_0\}} \{x_i : x_i \text{ randomly selected in } \Phi_c(y)\}.$$

At the intended collector, the total interference power is,

$$I(o) = \sum_{x_i \in \Phi_i} P_t \; \alpha \; |x_i|^{-\beta} \; A_{f,i}.$$

The set of interfering nodes Φ_i is illustrated in Figure 2. This set cannot be considered as homogeneous PPP and its exact statistical distribution is generally a difficult problem to model. For this, we use the same approximation proposed in [4] that is shown to almost capture the statistical behavior of the interference field. We let

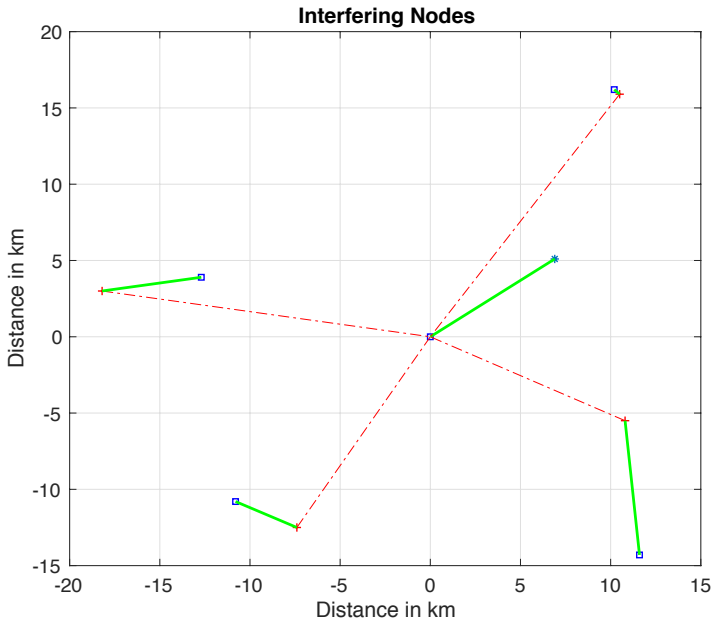

Figure 2: There is only one interfering node per cell. The useful signals are illustrated by the green line. The interfering signals are illustrated by red dashed lines. The set of interfering node can be approximated by an heterogeneous PPP with intensity $\lambda(x) = \lambda_b(1 - e^{-\lambda_b \pi |x|^2})$.

d_i be the distance between the interferer and the intended collector. The probability of finding at least one collector in the ball with radius d_i centered at the interferer is $(1 - e^{-\lambda_b \pi d_i^2})$. In this case, a node at distance d_i from the intended collector is considered as interfering with probability of $(1 - e^{-\lambda_b \pi d_i^2})$. It was shown in [4], that the effective interference observed at the tagged collector can be approximatively modeled as a non-homogeneous PPP with intensity $\lambda_b(1 - e^{-\lambda_b \pi d_i^2})$. The interference Laplacian is therefore,

$$\mathcal{L}_I(s) = \mathbb{E}\left[e^{-s\,I}\right] = \mathbb{E}\left[\prod_{x_i \in \Phi_I} e^{-sP_t\,\alpha\,|x_i|^{-\beta}\,A_{f,i}}\right]$$

By averaging over the Rayleigh fading coefficients,

$$\mathcal{L}_I(s) = \mathbb{E}\left[\prod_{x_i \in \Phi_I} \frac{1}{1 + sP_t\,\alpha\,|x_i|^{-\beta}}\right].$$

Using the PGFL property, the Laplacian is then computed as,

$$\mathcal{L}_I(s) = \exp\left(-2\pi\lambda_b \int_0^\infty \left[\frac{sP_t\,\alpha\,u^{-\beta}}{1 + sP_t\,\alpha\,u^{-\beta}}\right](1 - e^{-\lambda_b \pi u^2})udu\right). \quad (1)$$

2.1.2 Typical cell average size

Let $\Phi_c(o)$ be a typical cell centered at the origin o. Let r_1 be the distance between a point $x \in \Phi$ and its nearest collector $\in \Phi_b \cup \{o\}$ and r be the distance between a

sensor node x and a collector $y \in \Phi_b \cup \{o\}$. The typical average size of the cell is,

$$\mathbb{E}\Big[|\Phi_c(o)|\Big] = \mathbb{E}\left[\sum_{x\in\Phi} \mathbb{1}_{\{|x|\leq r_1\}}\right]$$

Using Campbell theorem [5],

$$\mathbb{E}\Big[|\Phi_c(o)|\Big] = \int_0^R \int_r^\infty f(r_1)dr_1(2\pi\lambda_a r)dr$$

The typical average size of the cell is therefore,

$$\mathbb{E}\Big[|\Phi_c(o)|\Big] = \frac{\lambda_a}{\lambda_b}\Big(1 - e^{-\lambda_b \pi R^2}\Big).$$

2.2 Spatial PPP versus other processes

Table 1 lists and compare the different spatial processes that can be also used to model the LPWA network.

3 Statistical dimensioning of NB-IoT network

Given the density of collectors in the network, we provide in this section statistical tools to compute the required bandwidth that supports the target rate of R bps per active sensor node. We assume an OFDMA network access (LTE-like network), the Radio Resource (RR) corresponds to a time slot of 0.5 ms in a bandwidth of $B = 180$ kHz. We consider a communication on a like- Physical Uplink Shared Channel (PUSCH) that carries the UL user data. Our main objective here is to statistically determine the total number of RRs to minimize the occurrence of the network outage event. This event arises when the total number of RRs is higher than the number of RRs at the collector side.

For this, we define first in Subsection 3.1 the dimensioning objectives and provide in Subsection 3.1 a general expression of the first and second moment on total RR. Next, we compare the single antenna-collector case with the multi-antenna case in Subsections 3.2 and 3.3. Numerical results are provided in Subsection 3.4.

3.1 Dimensioning objectives in a typical cluster

In a typical cluster $\Phi_c(0)$ centered at the origin o, the collector o allocates according to the level of the received SINR, 1 to $N_{\max}$ Radio Resources (RR) to the sensor node in order to achieve its target data rate R. The required number of RR is therefore,

$$N_{RR}(x) = \sum_{k=1}^{N_{\max}} k \times \mathbb{1}_{\left\{\,\mathrm{SINR}(y,x)\,\in\,[\gamma_{k-1}\,;\,\gamma_k]\right\}} + N_{\max}\mathbb{1}_{\left\{\,\mathrm{SINR}(y,x)>\gamma_k\right\}}. \tag{2}$$

The sensor is individually in outage if,

$$\mathbb{P}_{\mathrm{out},i}(0, N_{\max}) = \mathrm{Prob}\{\mathrm{SINR}(0,x) < \gamma_k\}$$

Distribution	**Characteristics**
Regular Grid	The number of nodes is **fixed** and the nodes are placed on a given square or hexagonal **grid**. This process is suitable for scenarios in which the number of simultaneously transmitting sensors or receiving collectors is predefined in advance, which cannot be always feasible in a practical scenario.
Homogeneous PPP	The number of nodes is **random** and the distribution follows a **Poisson law** with **intensity** λ that is **independent** of the nodes positions. Given the random number of nodes, the nodes are **uniformly** distributed in the area. Unlike the regular grid case, the homogeneous PPP is more general and can be applied in a **beacon enabled network**, as well the case of a **non-beacon enabled** one. This process is suitable for smart parking, or a smart viticulture, etc use cases in D2.1 [16] where the number of simultaneously transmitting sensor is random. The homogeneous PPP is also suitable to model the automatic on/off switch of collectors.
Heterogeneous PPP	The number of nodes is **random** and the distribution follows a **Poisson law** with **intensity** that **depends** on the nodes positions. As it will be shown, this process is suitable to approximate the behavior of interfering nodes.
Mátern Process (MP)	The MP results from a **dependent thinning** of an homogeneous PPP in which two nodes are selected if the **distance** between them is **higher** than a given threshold δ. If $\delta \to 0$, the MP converges towards the homogeneous PPP. In the considered use cases in D.1.1., no minimal distance where imposed between collectors and if so, it can be considered as negligible.

Table 1: Comparison of Homogeneous PPP with other spatial point processes

The total of required RR in this typical cluster is,

$$N_{RR,t}(0) = \sum_{x \in \Phi_c(y_0)} N_{RR}(x).$$

The network is in outage if,

$$\mathbb{P}_{\text{out},c}(N_t) = \text{Prob}\{N_{RR,t}(0) > N_{\text{net},t}\}.$$

In order to ensure an optimized network dimensioning, one should jointly find: (i)- the maximal number of radio resources $N^*_{\max}$ to be allocated per sensor in order to target an individual outage probability of $p_{\text{th},i}$; (ii)- the optimal number of total radio resources N_t to target a network outage probability of $p_{\text{th},n}$. Using the concentration inequality, one can find an upper-bound on the typical cluster outage probability such that,

$$\mathbb{P}_{\text{out},c}(N_t) \leq \mathbb{P}_{\text{sup}}(N_t),$$

where

$$\mathbb{P}_{\text{sup}}(N_t) = \exp\left(-\frac{v_N}{N^2_{\max}} g\left(\frac{N_{\max}(N_t - m_N)}{v_N}\right)\right),$$

with

$$m_N = \mathbb{E}\Big[\sum_{x \in \Phi_c(o)} N_{RR}(x)\Big],$$

and

$$v_N = \mathbb{E}\Big[\sum_{x \in \Phi_c(o)} N^2_{RR}(x)\Big].$$

being the first and the second moment. By setting a threshold $p_{th,i}$ on individual node outage, $p_{th,n}$ on the network outage, then,

$$\begin{aligned} N^*_{\max} &= \arg\{\mathbb{P}_{\text{out},i} = p_{th,i}\}, \\ N^*_{\text{net},t} &= m_N + \frac{v_N}{N^*_{\max}} g^{-1}\left(\frac{N^{*2}_{\max}}{v_n} \log\left(\frac{1}{p_{\text{th},n}}\right)\right) \end{aligned}$$

General expression of the first and second moment

Considering the clustered LPWAN constraints, the expressions of m_N and v_N are

$$\begin{aligned} m_N &= \frac{\lambda_a}{\lambda_b}\, \mathbb{E}_r\, \mathbb{E}_I\, \mathbb{E}_{A_f}[N_{RR}(r, A_f, I)], \\ v_N &= \frac{\lambda_a}{\lambda_b}\, \mathbb{E}_r\, \mathbb{E}_I\, \mathbb{E}_{A_f}[N_{RR}(r, A_f, I)]. \end{aligned}$$

The derivation details are provided in Appendix B. By replacing $N_{RR}(r)$ by (2),

$$m_N = \frac{\lambda_a}{\lambda_b} \sum_{k=1}^{N_{\max}} k\, \mathbb{E}_r\, \mathbb{E}_I\, \mathbb{E}_{A_f}[\mathbb{1}_{\{A_{f,k-1} \leq A_f < A_{f,k}\}}] + \frac{\lambda_a}{\lambda_b}\, N_{\max}\, \mathbb{P}_{\text{out},i}(o), \tag{3}$$

with

$$\mathbb{P}_{\text{out},i}(o) = \mathbb{E}_r\, \mathbb{E}_I\, \mathbb{E}_{A_f}[A_f < A_{f,N_{\max}}]$$

being the individual outage probability, and,

$$A_{f,k} = \gamma_k \alpha^{-1} r^{\beta} (N + I),$$

being the threshold fading to achieve a rate $R_k \in [R/k\ ;\ R/(k-1)]$ over one RR, that is computed using the threshold SINR γ_k. In a similar way, the second moment is,

$$v_N = \frac{\lambda_a}{\lambda_b} \sum_{k=1}^{N_{\max}} k^2\ \mathbb{E}_r\ \mathbb{E}_I\ \mathbb{E}_{A_f}[\mathbb{1}_{\{A_{f,k-1} \leq A_f < A_{f,k}\}}] + \frac{\lambda_a}{\lambda_b}\ N_{\max} \mathbb{P}_{\text{out},i}(o). \tag{4}$$

3.2 Case of single antenna receiver

Using a single antenne receiver, the SISO fading coefficients are Rayleigh distributed and A_f has an exponential distribution. This means that,

$$\text{Prob}\{A_f \leq u\} = (1 - e^{-u}).$$

Using the expression of m_N in (3),

$$\mathbb{E}_{A_f}[\mathbb{1}_{\{A_{f,k-1} \leq A_f < A_{f,k}\}}] = e^{-(N+I)s_{k-1}} - e^{-(N+I)s_k},$$

with $s_k = \text{SINR}_k\, \alpha^{-1} r^{\beta}$. The interference laplacian $\mathcal{L}_I(.)$ can be computed using (1). Consequently,

$$m_N = \frac{\lambda_a}{\lambda_b} \sum_{k=1}^{N_{\max}} k\ \mathbb{E}_r\Big[\mathcal{L}_N(s_{k-1})\mathcal{L}_I(s_{k-1}) - \mathcal{L}_N(s_k)\mathcal{L}_I(s_k)\Big] + \frac{\lambda_a}{\lambda_b}\ N_{\max}\ \mathbb{P}_{\text{out},i}(o). \tag{5}$$

Similarly,

$$v_N = \frac{\lambda_a}{\lambda_b} \sum_{k=1}^{N_{\max}} k^2\ \mathbb{E}_r\Big[\mathcal{L}_N(s_{k-1})\mathcal{L}_I(s_{k-1}) - \mathcal{L}_N(s_k)\mathcal{L}_I(s_k)\Big] + \frac{\lambda_a}{\lambda_b}\ N_{\max}^2\ \mathbb{P}_{\text{out},i}(o). \tag{6}$$

3.3 Case of multi-antenna receiver

We assume SIMO configuration in which n_r antennas are used at the receiver and only a single antenna at each sensor node. Two transmission modes are considered: the first transmission is the antenna selection in which the transmission is performed on the path with highest fading coefficient. The second transmission is the Maximum Ratio Combiner, in which the received signals at the different antenna are combined using a MRC decoder.

3.3.1 Antenna selection

Using antenna selection, the fading coefficient is distributed as the maximum between n_r i.i.d exponential variables. This means that,

$$\text{Prob}\{A_f \leq u\} = (1 - e^{-u})^{n_r} = \sum_{p=0}^{n_r} (-1)^p \binom{p}{n_r} e^{-pu}$$

Consequently,

$$m_N = \frac{\lambda_a}{\lambda_b} \sum_{k=1}^{N_{\max}} k\, \mathbb{E}_r \sum_{p=0}^{n_r} (-1)^p \binom{p}{n_r} \Big[\mathcal{L}_N(ps_{k-1})\mathcal{L}_I(ps_{k-1}) - \mathcal{L}_N(ps_k)\mathcal{L}_I(ps_k)\Big] + \frac{\lambda_a}{\lambda_b} N_{\max}\, \mathbb{P}_{\text{out},i}(o). \quad (7)$$

Similarly,

$$v_N = \frac{\lambda_a}{\lambda_b} \sum_{k=1}^{N_{\max}} k^2\, \mathbb{E}_r \sum_{p=0}^{n_r} (-1)^p \binom{p}{n_r} \Big[\mathcal{L}_N(ps_{k-1})\mathcal{L}_I(ps_{k-1}) - \mathcal{L}_N(ps_k)\mathcal{L}_I(ps_k)\Big] + \frac{\lambda_a}{\lambda_b} N_{\max}^2\, \mathbb{P}_{\text{out},i}(o). \quad (8)$$

3.3.2 Maximum Ratio Combiner

Using a MRC, the fading coefficient is distributed as chi-squared random variable with $2n_r$ degrees of freedom. This means that,

$$\text{Prob}\{A_f \leq u\} = 1 - \sum_{p=0}^{n_r-1} \frac{1}{p!} u^p e^{-u}.$$

Using the expression of m_N in (3),

$$\mathbb{E}_{A_f}[\mathbb{1}_{\{A_{f,k-1} \leq A_f < A_{f,k}\}}] = \sum_{p=0}^{n_r-1} \Big[(N+I)^p s_{k-1}^p e^{-(N+I)s_{k-1}} - (N+I)^p s_k^p e^{-(N+I)s_k}\Big],$$

By averaging over the noise and the interference level,

$$m_N = \frac{\lambda_a}{\lambda_b} \sum_{k=1}^{N_{\max}} k\, \mathbb{E}_r \left[\sum_{p=0}^{n_r-1} \frac{1}{p!}\Big(\Xi_p(s_{k-1}) - \Xi_p(s_k)\Big)\right] + \frac{\lambda_a}{\lambda_b} N_{\max}\, \mathbb{P}_{\text{out},i}(o), \quad (9)$$

with

$$\Xi_p(s) = (-1)^p \sum_{j=0}^{p} s^p \binom{j}{p} \frac{\partial^j \mathcal{L}_N(s)}{\partial s^j} \frac{\partial^{p-j} \mathcal{L}_N(s)}{\partial s^{p-j}}.$$

Similarly,

$$v_N = \frac{\lambda_a}{\lambda_b} \sum_{k=1}^{N_{\max}} k^2\, \mathbb{E}_r \left[\sum_{p=0}^{n_r-1} \frac{1}{p!}\Big(\Xi_p(s_{k-1}) - \Xi_p(s_k)\Big)\right] + \frac{\lambda_a}{\lambda_b} N_{\max}^2\, \mathbb{P}_{\text{out},i}(o). \quad (10)$$

3.4 Numerical results

In this section, we consider a sensor network with parameters defined in Table 2. The proposed statistical model estimates the required number of RRs considering the whole space $\mathbb{R}^2$. In order to limit the complexity of the numerical computation of

Area radius	$R = 10$ km
Mean arrival rate	$\rho_a = 45$ nodes per hour per km^2
Mean time of service	10 s
Intensity of active nodes	$\lambda_a = 0.125$ nodes per km^2
Transmission Power	$P_t = 14$ to 21 dBm
RR per node	1 to 6 RRs
Target individual outage threshold	2×10^{-2}
Target typical cluster outage threshold	$< 10^{-2}$
Antenna configuration	SISO or 1×2 SIMO
Target data rate	At least 500 bps

Table 2: Network Parameters

the integrals, we limit the maximal distance between a node belonging to the typical cluster to $R_{\max} = 40$ km as well as interfering point and we use a step $\Delta r = 0.01$ km. We neglect the probability to find a cluster node beyond this limit, by checking that

$$\text{Prob}\{\text{dist}(0, x) < R_{\max}\} = (1 - e^{-\lambda_b \pi R_{\max}^2}) \to 1$$

We also assume that the interference induced by nodes beyond this limit is negligible. Table 3 gives the matching between the SINR range with the required number of RR to achieve a target rate of 500 bps. This data are derived from the Link Layer Simulation (LLS) provided in [17] on the Physical Uplink Shared Channel of LTE-Cat M.

RR per node	SINR range (dB)
1	[-20.6; $+\infty$[
2	[-22.6; -20.6[
3	[-23.6; -22.6[
4	[-23.7; -23.6[
5	[-23.9; -23.7[
6	[-25.1; -23.9[

Table 3: MCS table: SINR versus RR required to achieve R = 500 bps

Figure 3 illustrates the maximal number of required RR per node considering variable collectors intensities. We recall that the maximal transmitted power per RR is fixed to 14 dBm. We can see that by fixing an individual outage probability of 10^{-2}, 3 RRs are required in the SISO case, however only 1 RR is sufficient in the SIMO case to achieve the target rate with the predefined outage threshold. This means that

in the worst case in a SISO communication, the sensor should transmit with a power that is three times higher than the SIMO case. The SIMO communication reduces the energy consumption of the nodes and increase hence the battery life.

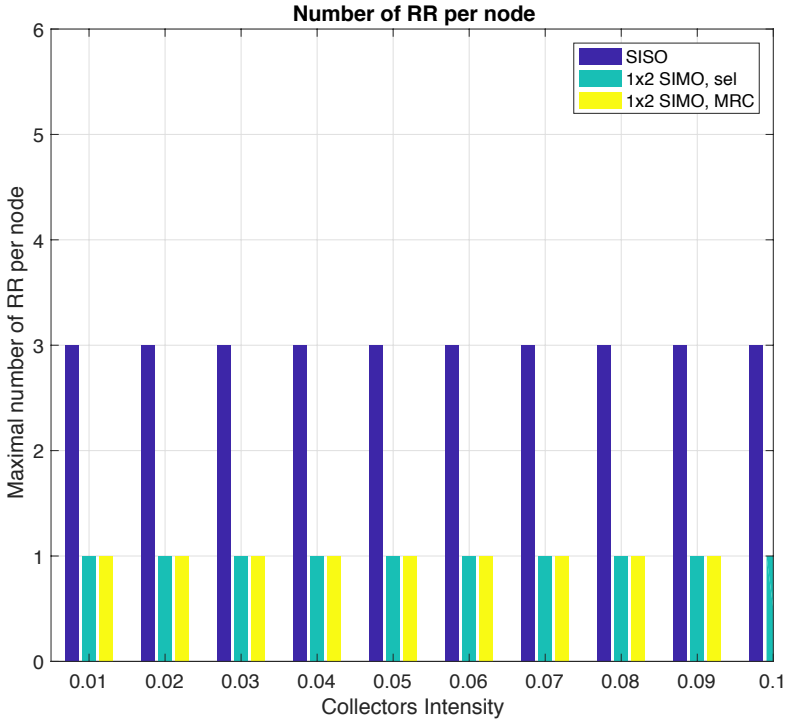

Figure 3: Maximal Required RR per Node

Figure 4 illustrates the mean number on required RR number in a typical cluster considering various collectors intensities. Increasing the intensity of the collectors, decrease the charge on the typical cluster, however, using a frequency pattern of one will increase the interference. For a large collector intensity, the mean number of nodes per cluster is very low, and even with high interference level, the SINR is sufficient enough to achieve the low target rate per node with a low number of RR.

Figure 5 illustrates the total number on required RR number in a typical cluster considering various collectors intensity. This number is computed using the mean number of RR and the second moment. As for the mean case, this number decreases when the collector intensity increases. A tradeoff between the bandwidth and the collector deployment should be thus found. Using a SIMO configuration minimizes statistically the required bandwidth as the receiver diversity enhances the level of SINR and decreases the number of required RR per node.

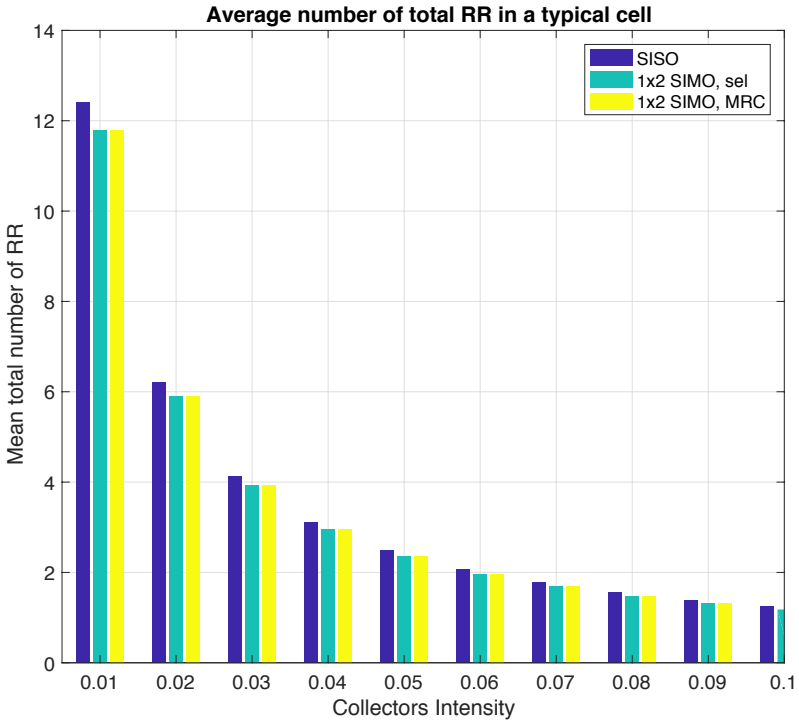

Figure 4: Mean Total number of RR in a Typical Cell

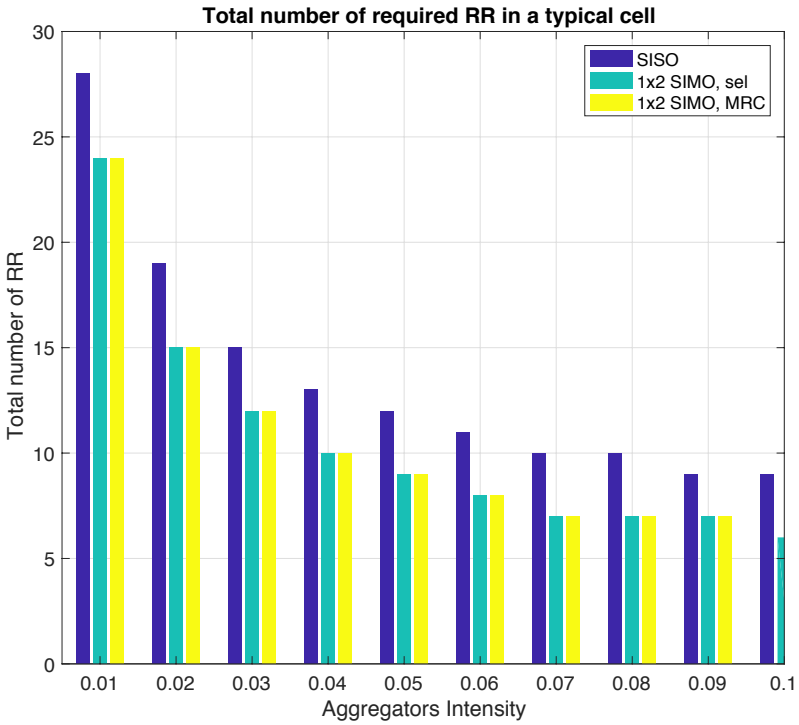

Figure 5: Required Total Number of RR in a Typical Cell

4 Enhancing coverage in NB-IoT using machine learning

In this section, we propose a new method to enhance the coverage based on machine learning. Instead of getting access to the spectrum in a random way, dynamic spectrum access based on reinforcement learning algorithms can help increasing the coverage, decreasing the number of repetitions, and thereby reducing the energy consumption. This problem can be modeled as multi-armed bandit (MAB) framework, as has been proposed for cognitive radio in the literature [18]. It has also been reported that MAB works well in real channel conditions [19]. One of the most relevant methods to address MAB problems is upper confidence band (UCB) algorithms, which are efficient and converge quickly when the traffic is stationary and independent and identically distributed [20]. Using this framework, the NB-IoT end device will select the best channel following not only the criterion of availability but also the best coverage condition.

Hereafter, we explain the NB-IoT challenges in terms of coverage enhancement and energy consumption, we show how can dynamic spectrum access and its tools enable to follow the requirements of NB-IoT. We also provides simulation results about our proposed solution.

4.1 NB-IoT Challenges

Enhancing the coverage and reducing the energy consumption are among the most relevant key targets of NB-IoT. In this section, we explain the challenges of increasing the coverage and saving energy as well as the recently deployed solutions to fulfill these main requirements.

4.1.1 Coverage enhancement

NB-IoT requires 20 dB of maximum coupling loss (MCL) higher than LTE, and then reaches up to 164 dB of MCL in order to serve end devices in deep coverage such as basements. Several modifications have been deployed on the different LTE protocol layers to achieve this significant gain. A major selected technique consists in increasing the number of retransmissions that reaches 128 repetitions for the uplink communications and 2048 for the downlink. These repetitions are combined at the receiver side in order to increase the signal-to-noise (SNR) ratio. Along with repeating the same transmission several times, other techniques have been used to extend the coverage such as cross-subframe channel estimation and frequency hopping. More details on these techniques can be found in [21].

Three coverage classes are allowed by a serving cell to an NB-IoT end device:

- CE level 0: normal coverage with MCL$\approx$ 144 dB and 15 kHz sub-carrier spacing
- CE level 1: robust coverage with MCL$\approx$ 154 dB and 15 kHz sub-carrier spacing
- CE level 2: extreme coverage with MCL$\approx$ 161 dB and 3.75 kHz sub-carrier spacing

The choice of the coverage level depends on the channel conditions. The extreme coverage level corresponds to a low power received level, and a normal coverage level corresponds to a high power received level. Each selected coverage class determines the transmission parameters including the number of repetitions. Such a deployment allows the UE to be served in different coverage conditions characterized by different ranges of path loss. Depending on the coverage level, the serving cell indicates to the UE to repeat the transmission $\{1, 2, 4, 8, 16, 32, 64, 128\}$ times, using the same transmission power on each repetition. Combining the different retransmissions allows a coverage extension.

4.1.2 Energy consumption

In addition to the normal connected mode, there are mainly two energy efficient techniques that have been designed in NB-IoT in order to minimize the power consumption in end devices and increase their battery life:

- Idle mode extended discontinuous reception (I-eDRX): this mode allows a discontinuous reception for maximum of 3 hours, which saves UE battery but still allows it to be reachable by the network through paging messages or downlink control channels.
- Power saving mode (PSM): this energy saving mode allows unconnected state for up to 13 days, where UE enters to a deep sleep. Unlike in I-eDRX, UE is unreachable while remains registered in the network. This mode saves more energy than the idle mode.

As expected, the power consumption of these modes is substantially lower than the power consumed during transmission. Therefore, in a normal environment conditions (MCL of 154 dB), configuration of these power saving techniques allows a battery life of more than 10 years. However, in deep indoor coverage conditions, the targeted level of battery life (more than 10 years) cannot be achievable since the uplink repetitions gets large. In addition, the energy consumption and the coverage enhancement mechanism imply high latency as the network waits a long period before being able to transmit its information data.

More techniques that allow both extending the coverage and reducing the number of required repetitions should be investigated to help prolong battery life. We show hereafter that dynamic spectrum access can help enhancing the coverage along with reducing the number of retransmissions and improving the latency.

4.2 Dynamic spectrum access can help

Instead of a random access based on slotted ALOHA which selects randomly the channel to sense in order to establish connection with the cell, we propose in this work to use a dynamic spectrum access in order to learn the channel which is more likely to be available and in a normal coverage conditions.

The spectrum learning process can be modeled as a multi-armed bandit (MAB) framework as proposed in [18, 22]. Depending on the location of UE (outdoor, indoor, basements) and the channel conditions (high or low SNR), the quality of the physical

channels changes. Therefore, choosing the channel with the best quality (i.e. coverage level), potentially leads to reliable transmissions, less costly in terms of energy consumption.

4.2.1 Multi-armed bandit framework

The MAB problem is a reinforcement learning game where a player have to decide which machine k to play (among K machines i.e $k \in \{0, 1, \ldots, K\}$) at each discrete time slot $t = 0, 1, 2 \ldots$, based on informations of their reward. The player plays the machine that has the maximum reward. The rewards associated to each machine k are independent and identically distributed (i.i.d.) and follows a fixed and unknown distribution law d_k. In general, the reward distributions $\{d_1, d_2, \ldots, d_K\}$ differ from one machine to another, and the player does not have any knowledge about these distributions.

In our case, the player is the NB-IoT end device, and the machines are the spectrum channels used for cell connection. In the following we define some concept related to the MAB framework.

Reward Let $r_t(k)$ be the reward of the data transmission for a channel k at instant t. The reward in our scenario takes two values 0 or 1. After sensing the channel with the best probability of availability and the best probability of good coverage, $r_t(k)$ is updated. In our scenario, we do not consider sensing errors [1] or acknowledgements [2]. We assume that the selected channel is generally associated to a good coverage, and the associated number of retransmissions is enough to deliver the information to the receiver.

Exploitation and exploration dilemma. It refers to a trade-off between the exploitation of the channel with highest reward, and exploring the other channels in order to get more information about their payoffs.

Regret. It means the loss represented by the difference between the expected reward associated to the suboptimal channel learned by the end device, and the ideal reward associated to the optimal channel. Since the user does not have any knowledge about the distribution of the reward, he cannot avoid a loss when selecting a channel.

Denote π the learning channels policy. Let $\mu_k = \mathrm{E}[d_k]$ the stationary mean reward of the k^{th} channel, where E[.] denotes the expectation function. The regret of a policy π is defined as

$$R_t^\pi = t.\mu^* - \sum_{l=0}^{t-1} r_l, \tag{11}$$

where μ^* stands for the expected value of the reward of the optimal channel.

Based on (11), we define the expected cumulated regret as

$$\mathrm{E}[R_t^\pi] = \sum_{k=1}^{K} (\mu^* - \mu_k)\mathrm{E}[T_k(t)], \tag{12}$$

[1] In [18], the authors analyses the impact of imperfect sensing in learning policies.

[2] In [23], authors consider the scenario where the end device waits for an acknowledgement before proceeding to another retransmission.

where $T_k(t)$ being the total number of times channel k has been sensed from instant 0 to instant $t-1$.

The MAB problem can be solved using reinforcement learning algorithms such as UCB approaches. In the following section, we briefly define the use of UCB in dynamic spectrum access.

4.2.2 Upper confidence bound algorithm

The policy that we seek should help the NB-IoT device to make a decision on which channel to transmit. We choose to build a policy based on the UCB algorithms since this approach requires few processing resources and memory, and guarantees asymptotically optimal performance. The upper confidence bound index $B_k(t)$, is computed at each instant t and for each channel k, and gives an estimation of the expected reward of a channel k. The UCB index is expressed as: $\mathbb{1}$

$$B_k(t) = \bar{X}_k(t) + A_k(t), \tag{13}$$

$$\text{such that} \quad \bar{X}_k(t) = \frac{1}{T_k(t)} \sum_{l=0}^{t-1} r_l(k) \mathbb{1}_{\{a_l=k\}} \tag{14}$$

$$A_k(t) = \sqrt{\frac{\alpha \ln t}{T_k(t)}}, \tag{15}$$

where $\bar{X}_k$ is the sample mean of the channel k reward, and A_k is an upper confidence bias. $\mathbb{1}$ is the indicator function and a_t is the selected channel using the policy π at the t^{th} transmission. Therefore, we have $\mathbb{1}_{\{a_l=k\}} = 1$ only if the channel k has been chosen for sensing at instant l. The factor α in (15) is an exploration coefficient for channel availability and coverage. If α gets larger, the UCB algorithm will explore more channels with good vacancy and coverage. Otherwise, when α takes lower values, the exploitation is privileged.

The selected channel a_t resulting from UCB algorithm is the one with the highest UCB index, i.e.

$$a_t = \arg\max_k (B_k(t)). \tag{16}$$

4.3 Simulation results

4.3.1 NB-IoT Scenario

NB-IoT standard designed by 3GPP is a slotted protocol [24]. We assume that the different communications using the studied spectrum are slotted i.e. all devices share synchronized time. We also assume that the end device knows in advance the finite number of available radio frequency (RF) channels.

The NB-IoT supports the following deployment modes:

- In-band mode where NB-IoT is deployed within the LTE bandwidth, and occupies one or multiple physical resource blocks (180 kHz).
- Guard-band mode where NB-IoT operates within the guard-band of an LTE carrier.

Table 4: LTE PRB indices allowed synchronization in for NB-IoT in-band deployment.

LTE bandwidth	3 MHz	5 MHz	10 MHz	15 MHz	20 MHz
LTE PRB indices for NB-IoT	2, 12	2, 7, 17, 22	4, 9, 14, 19, 30, 35, 40, 45	2, 7, 12, 17, 22, 27, 32, 42, 47, 52, 57, 62, 67, 72	4, 9, 14, 19, 24, 29, 34, 39, 44, 55, 60, 65, 70, 75, 80, 85, 90, 95

- Stand-alone mode where NB-IoT can either occupies one or more GSM carrier (200 kHz), or it can be deployed in an adjacent band to LTE.

It is worth mentioning that in the in-band deployment, the channels supported by NB-IoT are well-defined to avoid interfering with resources used by the LTE system such as synchronization, broadcast and control channels. The allowed physical resource blocks (PRB) are provided in Table 4. We assume in our scenario that the NB-IoT is deployed in in-band mode associated to LTE system bandwidth of 15 MHz. 14 physical channels are then allowed for cell connection as given by Table 4.

When the NB-IoT end device turns on, it starts searching for an available PRB to connect to the cell. The first part of the time slot is then reserved for the sensing operation, if the selected channel (following the UCB policy) is free, the device transmits the data during the second part of the slot. Otherwise, it waits till the beginning of the next slot to repeat the sensing operation and so on. At the end of each slot, the reward of the selected channel is updated.

We define μ^k_{vac} the expected mean reward associated to the vacancy of the PRBs k, and μ^k_{cov} the expected mean reward related to the coverage level of the PRBs k. Table 5 shows the values used in our learning policy, which are defined in a random way. Without loss of generality, we assume $\mu^1_{\text{vac}} \leq \mu^2_{\text{vac}} \dots \mu^{14}_{\text{vac}}$. Note that $\mu^1_{\text{vac}} = 10\%$ means that channel 1 is available 10% of the time.

4.3.2 Best channel selection and cumulated regret

In addition to the cumulated regret defined in Section 4.2.1, the percentage of optimal channel selection is a relevant metric in the analysis of reinforcement learning policies. Since the device should transmit in the optimal channel i.e. that has the highest mean reward, the more is the percentage of optimal channel selection, the better is the policy. Both of these relevant metrics are compared in Fig. 8, Fig. 6, Fig. 9, and Fig. 7 for the following proposed UCB scenarios:

- UCB(vac) means that the policy consider only the vacancy distributions μ^k_{vac} and assumes that the different channels have the same coverage properties. The best channel in this case is $14 = \arg\max_k(\mu^k_{\text{vac}})$. This scenario is extremely unlikely to happen, since the coverage level of each RF channel is independent from the probability of its availability.

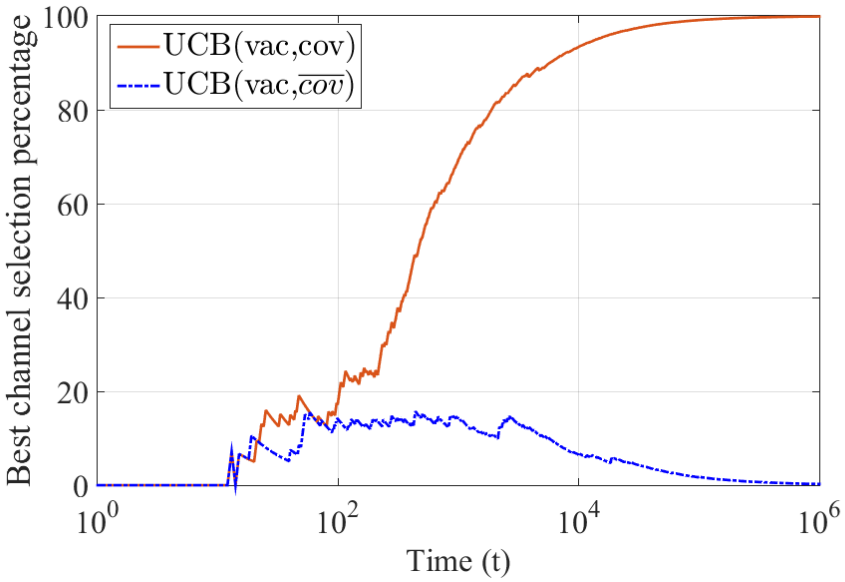

Figure 6: Impact of considering coverage on best channel selection percentage.

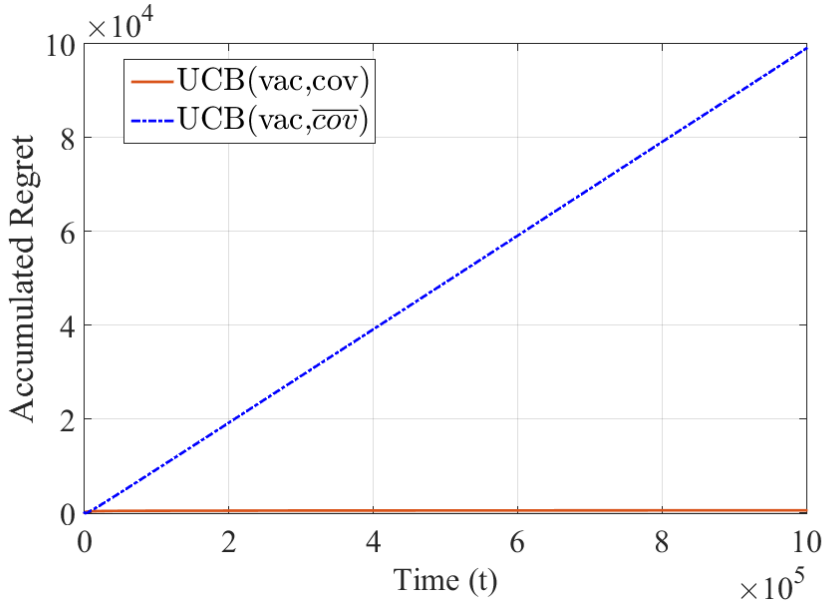

Figure 7: Impact of considering coverage on accumulated regret.

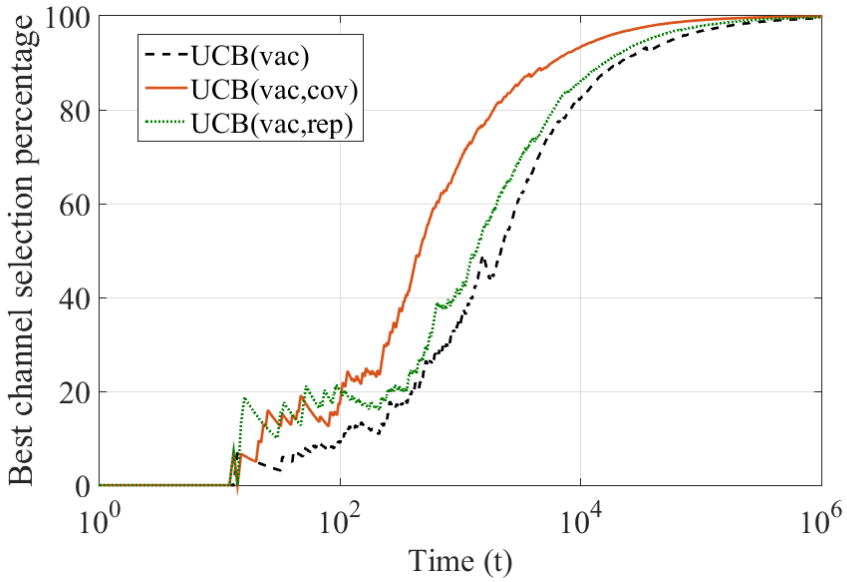

Figure 8: Best channel selection percentage for different scenarios.

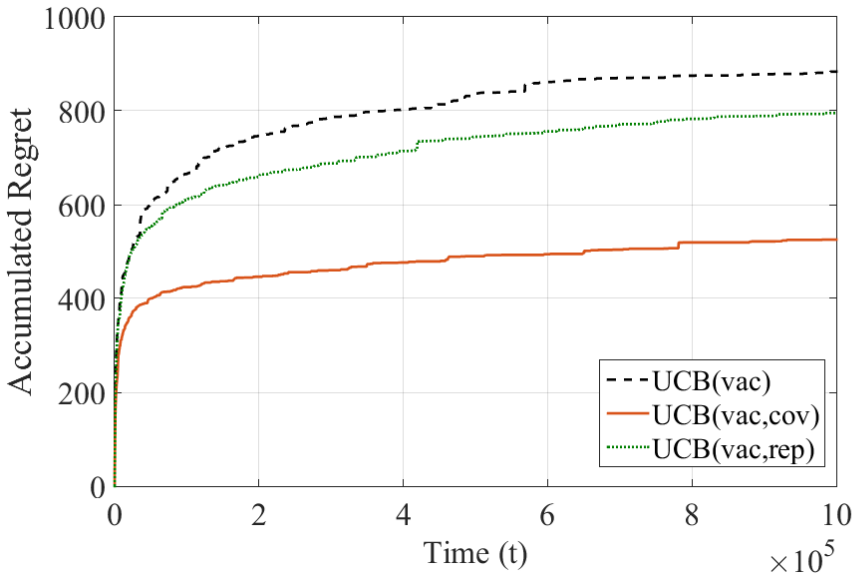

Figure 9: Accumulated regret for different scenarios.

Table 5: NB-IoT channel parameters for an LTE Bandwidth of 15 MHz when in-band mode is deployed.

PRB index	Channel index	μ^k_{vac} [%]	μ^k_{cov}	μ^k_{rep}	$\mu^k_{\text{vac,cov}} = \mu^k_{\text{vac}} \cdot \mu^k_{\text{cov}}$	$\mu^k_{\text{vac,rep}} = \mu^k_{\text{vac}} \cdot \mu^k_{\text{rep}}$
2	1	10	1	1/4	0.1	0.02
7	2	20	1/3	1/64	0.06	0.003
12	3	25	1/2	1/8	0.12	0.031
17	4	30	1/2	1/16	0.15	0.018
22	5	35	1/3	1/64	0.11	0.005
27	6	40	1/2	1/16	0.2	0.025
32	7	45	1/2	1/4	0.22	0.112
42	8	50	1/3	1/64	0.16	0.007
47	9	55	1	1/2	0.55	0.275
52	10	60	1/3	1/128	0.2	0.004
57	11	65	1/2	1/8	0.32	0.081
62	12	70	1/3	1/64	0.23	0.01
67	13	80	1	1/2	0.8	0.4
72	14	90	1/3	1/128	0.3	0.007

- UCB(vac,cov) takes into account both the vacancy and the coverage criteria. The policy is then based on the distribution $\mu^k_{\text{vac,cov}}$, which is inversely related to the coverage level. The best channel in this case is different from UCB(vac) case, and it corresponds to $13 = \arg\max_k(\mu^k_{\text{vac,cov}})$.

- UCB(vac,rep) considers the number of required repetitions rather than the coverage level along with the availability of the channel. $\mu^k_{\text{vac,rep}}$ is then the mean reward distribution considered in this case, which is inversely related to the number of repetitions. The best channel is the same as in UCB(vac,cov).

- UCB(vac,$\overline{\text{cov}}$): In this scenario, the channels do not have the same coverage level but follow the distributions μ^k_{cov}. However, the end device does not take the coverage criterion in the calculation of the UCB index [3], its calculation is based only on the vacancy distributions μ^k_{vac}. The best channel here is 13 since the channels have different coverage and vacancy properties.

The exploration coefficient α is set to 1.5 for all the studied scenarios.

Fig. 6 and Fig. 7 show the impact of the coverage constraint on the UCB policies. The major finding resulting from comparing the UCB(vac,$\overline{\text{cov}}$) policy where the coverage criterion is not considered, and the UCB(vac,cov) policy where the choice of the RF channel is constrained with its coverage quality, is that the former policy does not converge to the optimal channel unlike the latter. This result was expected from the behaviour and the target of each policy. During the first iterations, both algorithms

[3] This is what we mean by the notation $\overline{\text{cov}}$.

start exploring the physical channels with different objectives: UCB(vac,$\overline{\text{cov}}$) calculates its UCB index based on the mean reward of vacancy μ^k_{vac}, while UCB(vac,cov) takes into account both availability and coverage i.e. $\mu^k_{\text{vac,cov}}$ in its UCB index calculation. In the long run, UCB(vac,$\overline{\text{cov}}$) tends to choose the channel number 14, which is the most available one, while channel number 13 is the optimal one since it allows both a good availability and a good coverage level. The channel with the highest probability to be free is not necessarily the one with the best coverage. Therefore, the two compared policies behave in a symmetric manner, the best channel selection percentage decreases with time for UCB(vac,$\overline{\text{cov}}$) and tends to 0% while it converges to 100% for UCB(vac,cov) (see Fig. 6). The resulting accumulated regret increases linearly with time for UCB(vac,$\overline{\text{cov}}$) and seems insignificant for UCB(vac,cov) compared with the first policy (see Fig. 7). Note that in some other scenarios, the most available channel might be also the one with the best coverage level. Assuming this scenario, even if it is highly unlikely to occur, the policy UCB(vac,$\overline{\text{cov}}$) would not behave better than the proposed policy UCB(vac,cov).

We compare in Fig. 8 and Fig. 9 the previously analysed UCB(vac,cov) policy, with UCB(vac,rep) and UCB(vac) scenarios. It can be noticed that UCB(vac,cov) still gives the best performance. The algorithm converges faster than the others and produces the lowest accumulated regret. The UCB(vac,rep) scenario provides faster convergence than UCB(vac). As an example, if we consider the transmission i.e iteration number $t = 10^3$, the best channel selection associated to UCB(vac,cov) reaches 69.4%, while it is equal to 41.6% for UCB and to 34.4% for UCB(vac) which is less than half the percentage achieved by UCB(vac,cov). Regarding the accumulated regret, Fig. 9 reflects in fact the same performance behaviour. In order to give a numerical insight, let us consider another interval of the data transmission: $t = 10^5$. The accumulated regret corresponding to UCB(vac,cov) is only 424.4, while it reaches 609.5 for UCB(vac,rep) and 665.2 for UCB(vac).

Note that for the different scenarios, their behaviour during the first iterations is not regular. This is due to the random selection of the channels during the first round since no knowledge about the vacancy nor the coverage is available during the beginning of the iterations.

4.3.3 Coverage extension and reducing repetitions

In the previous section, we have strongly supported that integrating the coverage level constraint into the UCB policy improves the best channel selection percentage and decreases the accumulated regret. Regarding the studied scenarios that are associated to the distributed values reported in Table 5, using UCB(vac,cov) would rather choose a RF channel (channel number 13 in the provided example) with a normal coverage (CE level 0) that allows reaching easily the destination, than a RF channel (channel number 14) with an extreme coverage (CE level 2) that makes reaching the receiver pretty hard. Moreover, UCB(vac,rep) allows avoiding transmission repetitions by selecting a good quality channel that requires no or few number of repetitions. To support this claim, we can refer to the considered scenarios in the previous section which show that selecting the channel number 13 instead of channel number 14 reduces the number of repetitions from 128 to 2 times.

When using a random selection procedure, the channel to sense is chosen in a

random way, ignoring its probability of availability or its coverage/repetition properties. In the literature, several researchers have been defending the interest of dynamic spectrum access using the vacancy criterion of the channels. Here, we support the relevance of involving the quality of the channels in terms of coverage level and the number of repetitions in UCB policies, especially for applications that need a long battery lifetime such as NB-IoT. To be convinced of this, let us consider the best and worse case scenarios for the proposed policies UCB(vac,cov) and UCB(vac,rep):

- Best case scenario for implementing UCB proposed policies: the selected channel by a random selection procedure is the one with the highest required number of repetitions 128 (in an extreme coverage), while the optimal channel in UCB policy requires only 1 (or 0) repetition. This scenario would reduce the latency and save significant amount of energy by avoiding large number of retransmissions.
- Worse case scenario: the randomly selected channel matches the one with the best quality of service. This means that our policy for this typical transmission time, would not save a priori more energy than legacy selection schemes.

Hence, our policy promises in the general case a considerable improvement of the quality of the transmission, and meets then the challenges required by NB-IoT applications.

5 Improving reliability and latency using compressive sensing

New access techniques are needed in particular to meet the strong reliability and latency constraints in the context of Ultra Reliable Low Latency Communications (URLLC) in context of IoT. Here-under, we propose a model of Compressive Sensing-based communications as a good candidate of Non Orthogonal Multiple Access (NOMA) schemes for fulfilling those requirements.

In this section, we use the following notations:

- a is a scalar;
- $\mathbf{a}$ is a vector; $\mathbf{a}^T$ is the transposed vector.
- A is a matrix.

5.1 General model of the CS-based communication

5.1.1 Model definition

Consider sporadic simultaneous Low Power Wide Area Uplink communications between N transmitters and a receiver, where N is large. We note $\mathcal{N}$ the set of nodes. Let n denote one of the N sources, and $\mathcal{A}$ the subset of active nodes at a given slot. These nodes are supposed to be synchronous and transmit simultaneously complex signals $\mathbf{s^{(n)}}$ of size m. y is the observed signal at the single receiver; $H^{(n)}$ denotes the channel matrix of user n and $\mathbf{z}$ the additive white Gaussian noise. The received signal

can be expressed by the following equation:

$$\mathbf{y} = \sum_{n \in \mathcal{A}} H^{(n)} \mathbf{s^{(n)}} + \mathbf{z} \tag{17}$$

For example, with the assumptions of using m perfect discrete memoryless channels and having a single antenna at the receiver, (17) becomes

$$\mathbf{y} = \sum_{n \in \mathcal{A}} \begin{bmatrix} h_1^{(n)} & 0 & .. \\ 0 & h_2^{(n)} & 0 \\ .. & & \\ 0 & .. & h_m^{(n)} \end{bmatrix} \mathbf{s^{(n)}} + \mathbf{z}$$

The receiver aims to detect and recover each of the incoming signals. One could then call on a Multiple Access Channel technique, such as the TDMA, FDMA, CDMA, to enable this recovery operation. Those aforesaid techniques have a property of orthogonality in common, i.e. the devices communicate with orthogonal granted radio resources such that the signals do not overlap with each other. Taking the example of orthogonal codes, the modeling of user n transmission can be denoted by :

$$\mathbf{s^{(n)}} = \mathbf{c^{(n)}} x^{(n)}$$

where $\mathbf{c^{(n)}}$ is a coding sequence of size m allocated to user n and orthogonal to $\mathbf{c^{(j)}}$ $\forall j \in [1; N] \setminus \{n\}$; $x^{(n)}$ is the symbol to be sent. To fulfill the orthogonality while all nodes can transmit with some probability, the system requires $m \geq N$, which implies that the radio resources consumption increases within the same order of the transmitters' number N increase. Therefore, this criteria can not stand with a large N and the assumption of low power and low latency communications, which requires the latter to be as short as possible. One will then consider non orthogonal communications. In this case, the codes $\mathbf{c^{(n)}}$ are chosen as pseudo-orthogonal codes usually with a random noise generator. The model of non orthogonal transmissions is thus denoted by:

$$\mathbf{y} = \sum_{n \in \mathcal{A}} H^{(n)} \mathbf{c^{(n)}} x^{(n)} + \mathbf{z}. \tag{18}$$

Assuming knowledge of all $H^{(n)}$ and $\mathbf{c^{(n)}}$, $\mathbf{y}$ is a vector of m linear combinations, from which the unknown inputs $x^{(n)}$ are to be retrieved. Without a priori about the active subset $\mathcal{A}$, the receiver sees the system as :

$$\mathbf{y} = \sum_{n=1}^{N} H^{(n)} \mathbf{c^{(n)}} x^{(n)} + \mathbf{z}.$$

If the receiver seeks for a solution of $\mathbb{C}^N$, with $m \leq N$, the linear system is therefore under-determined and has an infinite number of solutions. However, one can exploit the sporadic property of the communications in order to provide the problem a significant hint. Indeed, since the communications occur sporadically, the solution is in $\mathbb{C}^k$ with $k = dim(\mathcal{A})$. This property, referred to as sparsity, is used when a set of elements is assumed to have a lot of zero elements compared to its dimension. For example, the

set $\mathcal{X} = \{x^{(n)}, \forall n \in \mathcal{N}\}$ is k-sparse (or has a sparsity level k), namely, the set $\mathcal{X}$ has k non-zero, or sparse, elements.

Under the assumption of sparsity, it is then possible to recover the information reliably even for $m \leq N$. The fundamental question addressed in this case is the trade-off between the code-length and the reliability as a function of the sparsity level.

But in a more general framework, each node may want to transmit more than one symbol and then aim at transmitting a codeword of size d. This is a straightforward extension of the former problem, where each source is a vector, noted $\mathbf{x^{(n)}}$, and the coding sequence is replaced by a coding matrix, leading to:

$$\mathbf{s^{(n)}} = C^{(n)}\mathbf{x^{(n)}}, \tag{19}$$

where $C^{(n)}$ is a complex coding matrix of size $m \times d$ allocated to user n; $\mathbf{x^{(n)}}$ is its signal of size d.

For a single antenna at the receiver, the observed signal $\mathbf{y}$ can be generalized by:

$$\mathbf{y} = HC\mathbf{x} + \mathbf{z} = \begin{bmatrix} H^{(1)} & .. & H^{(k)} \end{bmatrix} \begin{bmatrix} C^{(1)} & & 0 \\ & .. & \\ 0 & & C^{(k)} \end{bmatrix} \begin{bmatrix} \mathbf{x^{(1)}} \\ .. \\ \mathbf{x^{(k)}} \end{bmatrix} + \mathbf{z}, \tag{20}$$

where

- H, the concatenation of the channel matrices $H^{(n)}$, is a $m \times mk$ matrix;
- C is the $mk \times dk$ coding matrix;
- $\mathbf{x}$ is the input vector of size dk : $\mathbf{x} = [\mathbf{x^{(1)}}^T .. \mathbf{x^{(n)}}^T .. \mathbf{x^{(k)}}^T]^T$.

Note that for a α-antennas receiver, $H^{(n)}$ is a $\alpha m \times m$ matrix, then H size is $\alpha m \times mk$ and $\mathbf{y}$ is a αm vector, leading to :

$$\mathbf{y} = \begin{bmatrix} y_1 \\ . \\ . \\ y_{\alpha m} \end{bmatrix} = HC\mathbf{x}+\mathbf{z} = \begin{bmatrix} h_{1,1}^{(1)} & .. & h_{1,m}^{(1)} & .... & h_{1,1}^{(k)} & .. & h_{1,m}^{(k)} \\ & .. & & .... & & .. & \\ & .. & & .... & & .. & \\ h_{\alpha m,1}^{(1)} & .. & h_{\alpha m,m}^{(1)} & .... & h_{\alpha m,1}^{(k)} & .. & h_{\alpha m,m}^{(k)} \end{bmatrix} \begin{bmatrix} C^{(1)} & & 0 \\ & .. & \\ 0 & & C^{(k)} \end{bmatrix} \begin{bmatrix} \mathbf{x^{(1)}} \\ .. \\ \mathbf{x^{(k)}} \end{bmatrix} + \mathbf{z}$$

5.1.2 Parameters' hypotheses

We list here assumptions on the different variables of the equations (17) and (20) that impact their formulations:

- Channel matrix H
  The following cases are valid for both mono and multi-antennas receiver.
  - memoryless channels (MC): $H^{(n)}$ can be expressed by a diagonal matrix $diag(\mathbf{h^{(n)}})$;

  - channels with inter-symbol interference: $H^{(n)} = \begin{bmatrix} h_1^{(n)} & i_{12}^{(n)} & .. & i_{1m}^{(n)} \\ i_{21}^{(n)} & h_2^{(n)} & .. & \\ : & & & \\ i_{m1}^{(n)} & .. & & h_m^{(n)} \end{bmatrix}$;
  - stationary channels: the channels are coherent during the transmission t i.e. $h_{ii}^{(n)} = cst\ \forall i \in [1; m]$. When the m radio resources are seen as time slots of the transmission t, $H^{(n)} = h^{(n)}.I_m$ under memoryless channels assumption;
  - flat fading: $H^{(n)}$ is a vector; if the channel combines flat fading with memoryless and stationary properties, $H^{(n)}$ is represented by a single scalar $h^{(n)}$ and is named block fading.

- Noise vector $\mathbf{z}$
  Gaussian noise : $\mathbf{z} \backsim \mathcal{N}(0, \sigma^2)$.

- Coding matrix C can be one of the following

  - $m \times k$ matrix of Pseudo-Noise sequences;
  - $m \times k$ Gaussian matrix of normalized columns: $c_{ij} \backsim \mathcal{N}(0, 1/m)$;
  - $mk \times dk$ matrix of coding matrices with i.i.d elements.
  - $mk \times dk$ matrix of resource allocation matrices (i.e. with binary elements on its diagonal).

- Input $\mathbf{x^{(n)}}$ can be either a scalar:

  - binary bit,
  - symbol,

  or a vector:

  - binary sequence,
  - symbol sequence.

5.2 Problem formulation

In the literature, the model (17) and its generalization (20) are used for two kinds of problems :

- the objective is to detect the active nodes, and not to decode the content of $x^{(n)}$ ([25, 26, 27, 28]). In this case the error criteria is measured by the missed-detection or false-detection statistics.

- the objective is to decode the information sent by the sources, directly coded by $x^{(n)}$ (e.g. a binary information, or M-ary information) ([29];[30];[31]).

In either case, as stated previously, a trade-off must be found for optimizing the reliability, as the number of simultaneous successfully detected and estimated messages, while keeping the messages length (so the latency) and power as low as possible.

5.3 State of the art

Both the detection and the estimation problems have been studied in the literature. Fletcher et al. in [26] and [25] have focused on the detection problem : they proposed a CS framework for On-Off random communications and a theoretical analysis of necessary and sufficient conditions for a reliable detection in the asymptotic regime (i.e. when the number of nodes $N \to \infty$).

[26] draws the parallel between an on-off random communication scheme and the mathematical problem of sparsity detection in CS : it considers N users willing to transmit to the same receiver with a probability λ using a codebook of m degrees of freedom and of Gaussian elements. The signal sent by the N users can be represented by a vector whose each element corresponds to a user. If the user is active since it transmits with a probability λ (communication On), its element will be a non-zero value whereas the inactive users (communication Off) will be assigned a zero in the vector. Therefore, the vector illustrates the random On-Off communications, and recovering the locations of the non-zero elements is then identifying the set of active users. The main assumptions thus include a single symbol transmission per node, a perfect synchronization, complex Gaussian distributions for the components of the codebook (i.e. the matrix C in (20))and the noise $\mathbf{z}$. The channels correspond to memoryless channels with m-block flat fading conditions. For a particular node, the unknown input $x^{(n)}$ therefore corresponds to the product of the single modulated symbol and the channel gain.
Fletcher et al. analyze and compare the necessary and/or sufficient conditions on m depending on the SNR and power allocation conditions for the sparsity pattern recovery of a large range of detection algorithms such as Maximum Likelihood (ML), Single User Detection, Orthogonal Matching Pursuit (OMP), Least Absolute Shrinkage and Selection Operator (LASSO), Sequential OMP and the Thresholding algorithm -the last two algorithms being their own propositions for these studies-. In particular, despite its lower performance compared to usual OMP, SeqOMP is used to show the efficiency of an optimal power shaping. This optimization is determined by maximizing the minimal value of SINR γ

$$\gamma \approx \frac{1}{\lambda N} \log(1 + SNR),$$

for large N. The set of power allocated to user n is

$$p_n = \gamma(1 + \lambda\gamma)^{N-n},$$

for $n \in [1, N]$ and corresponds to the optimal power allocation of the MAC with a SIC detector. With this exponential power shaping, the sufficient condition for asymptotic reliable detection is :

$$m \geq 5\lambda N,$$

so that for SeqOMP m is in the order of ML asymptotic scaling law at high SNR ($m \geq \lambda N$).

Ji et al. in [27], as well as Wunder et al. in [32], have studied the joint users detection and data estimation problem. More specifically, [32] deals with the joint

activity, channel and data estimation. Contrary to the works of Fletcher et al., the receiver seeks for data sequences (instead of the users activity states). Both articles consider coded slotted Aloha communications, with replicas (on top of FDMA resources for [32]). Their objective is rather oriented to a throughput evaluation, to define an optimal resource load and to maximize the user achievable rate of the system respectively.

More precisely, [27] considers a coded slotted and replicated Aloha access using Pseudo Noise sequences for a high density of nodes. A synchronization is assumed at the slot level thanks to beacons broadcast by the Base Station. The algorithm performing the joint detection and estimation is a GroupOMP, since it is dedicated to detect and estimate groups of m symbols in case of active users. The evaluation of the asymptotic probability of users transmission recovery (when $N \rightarrow \infty$) is derived from the probability of recovering one of the replicas at a user side and the probability of recovering a replica of one of the users' transmissions at the slot side. The global probability of transmission recovery in the model case can be obtained by introducing the probability of recovering users transmissions via CS-Multi User Detection. 3 performance criteria are then evaluated : the maximum user resolution probability, the maximum expected throughput (as a function of the users detection), and the optimum average slot degree (which is defined as the number of users transmissions in a slot). The results show that CS can improve detection of coded random access.

In the work of [32], considering coded Aloha on FDMA, a message consists of a preamble as a user signature, also indicating the resource pattern, and a modulated data sequence. An Additive White Gaussian Noise and fast fading channels are assumed. A coding matrix fulfilling the CS theory constraint is employed. The joint user activity and channel estimation is performed via Basis Pursuit or greedy algorithm thanks to the preamble. The data is then decoded with interference cancellation based on an iterative belief propagation algorithm,which provides the probability of successfully decoded users. An evaluation of the users rates is given, taking into account the expectation on the fast fading channel realization, the dimension of the preamble, the noise distribution parameter, the ratio of power allocation between control and data parts.

[30] also provides a solution for small packets communications, based on the Compressive Sensing theory. This work includes a coding NOMA technique and its evaluation for both detection and estimation problems. We detail this study below.

5.3.1 Many access for Small Packets Based on Precoding and Sparsity-Aware Recovery [30]

The solution proposed in this article contributes to solving the problem of excessive signaling faced by small packets communication in current networks. The proposition is based on a Non Orthogonal Multiple Access technique for a multi-antenna Base Station system and on a new detection algorithm. It combines block precoding at the transmitters for multiuser transmissions, and sparsity aware recovery at the BS for joint detection and demodulation : an improved normalized block-OMP algorithm (N-BOMP and ICBOMP). The analysis is an approximate statistical evaluation of the Group User Detection Success Rate and of the SER, using order statistics. The real performances retrieved from simulations are also shown in the paper. The simulations

compare the algorithm propositions to the original algorithm, and to the approximate analysis of the solution, both in terms of GUDSR and SER.

The model considers a block sparsity pattern, where a block corresponds to a message, and the sparsity level N_a (i.e. the number of simultaneous messages or active users among the total N) is unknown but bounded by a maximum value $N_{a\ max}$. A Gaussian noise and a block fading model are included, the channel remaining coherent during m symbols, i.e. the frame size. The users are synchronized at a frame (or block) and symbol levels but there is no other coordination with the BS. The channels $h_i^{(n)}$ between the user n and the BS antenna $i \in [1; \alpha]$ are spatially independent. A perfect CSI at the BS is assumed for all the users and the BS antennas.

The precoding is achieved by the column-normalized matrix $P^{(n)} \in \mathbb{C}^{m \times d}$ where d is the initial size of the data $\mathbf{s^{(n)}}$ of the user n. $P^{(n)}$ is specific to the node n. The obtained message $\mathbf{x^{(n)}}$ is a block of m symbols, i.e. the symbols vector $\mathbf{x^{(n)}} = P^{(n)}\mathbf{s^{(n)}}$.

The received signal $Y \in \mathbb{C}^{\alpha \times m}$ (with α the number of the BS antennas) can be expressed by

$$Y = \sqrt{\rho_0} \sum_{n=1}^{N_a} \mathbf{h^{(n)}} \mathbf{x^{(n)}}^T + Z, \tag{21}$$

where ρ_0 is the SNR, for a user n $\mathbf{h^{(n)}} \in \mathbb{C}^{\alpha}$ is the vector of the channel response coefficients for the α antennas, $\mathbf{x^{(n)}}^T$ the transpose symbols vector of length m after precoding and $Z \in \mathbb{C}^{\alpha \times m}$ the noise. After vectorization, which makes the block sparsity model apparent, the vectorized received signal matrix Y is denoted by $\mathbf{y} \in \mathbb{C}^{\alpha.m}$:

$$vec(Y) = \mathbf{y} = \sqrt{\rho_0} \sum_{n=1}^{N_a} (P^{(n)} \otimes \mathbf{h^{(n)}})\mathbf{s^{(n)}} + \mathbf{z} = \sqrt{\rho_0} \sum_{n=1}^{N_a} B^{(n)}\mathbf{s^{(n)}} + \mathbf{z},$$

$$\mathbf{y} = \sqrt{\rho_0} B\mathbf{s} + \mathbf{z}, \tag{22}$$

where $\otimes$ denotes the Kronecker product, B the concatenation of the node matrix signatures $B^{(n)}$, $\mathbf{s}$ the unknown and block-sparse data vector, having N_a blocks of d non-zero variables among its Nd entries, and $vec(Z) = \mathbf{z}$. The model also includes the assumptions of Gaussian distributions for entries of the data vector $\mathbf{s}$, channels vectors $\mathbf{h^{(n)}}$, noise $\mathbf{z}$, precoding matrices $P^{(n)}$, signature matrices $B^{(n)}$.

Based on the block sparsity assumption, the algorithm chosen for the joined detection and estimation is a Block Orthogonal Matching Pursuit (BOMP). The BOMP iterates $N_{a\ max}$ loops including :

- for each undetected node, the correlation between the residual received signal and the node matrix signatures are computed.
- the node having the strongest correlation coefficient is selected.
- the messages corresponding to the selected nodes set are estimated with Least Square algorithm.
- the estimated messages contributions from the received signal are excluded, leading to an updated residual received signal to be evaluated at next iteration.

Apart from the proposition of this NOMA technique exploiting a block sparsity model for small packets communications, and its complete description, the contributions of this paper also include 2 other algorithms called N-BOMP and ICBOMP, aiming at improving the BOMP performances. The authors provide the theoretical analysis of N-BOMP and both of them are evaluated by simulations.

The first proposition is a Normalized BOMP (N-BOMP), using the channels knowledge assumption for removing the strong or weak channel effect on the correlation operation. Indeed, for each node, its correlation coefficient is normalized by the channel gain. The theoretical analysis of this algorithm is detailed below.

The ICBOMP algorithm (where IC stands for Interference Cancellation) performs user detection, message estimation in addition to error correction and detection at each round (a Cyclic Redundancy Check code and an error correction code have been employed). For this second proposition, once the signal from one detected user is correctly decoded, it is removed from the set of detected signals to be estimated by the least square algorithm, which saves some computational cycles since it is not re-evaluated in the following iterations. Perfect interference cancellation realized with those particular signals reduces error propagation, as the simulations show a lower Symbol Error Rate with ICBOMP.

The theoretical analysis of the N-BOMP successful recovery (including detection and signals reconstruction) is based on approximating the most likely successful detection case probability. The detection performance is then evaluated with a lower bound of the Group User Detection Success Rate. The signal reconstruction performance is evaluated by the Symbol Error Rate.

From the means and variances of correlation coefficients (used in the N-BOMP algorithm for discriminating the active users among N) of the active and inactive groups, and using order statistics of the channels gains, the PDF of correlation coefficients for both active and inactive users can be computed. It leads to the probability of the detection success, since the latter can be approximated by the events where the correlation coefficient of the active node to be detected at the current iteration is greater than any correlation coefficient of inactive nodes. The detection performance of N-BOMP is therefore described by the approximation of a lower bound of the Group User Detection Success Rate :

$$GUDSR \approx \prod_{k=1}^{N_a} \int_{-\infty}^{+\infty} \Big[\int_{-\infty}^{x_1} f_{0,k,max}(x_0) dx_0 \Big] f_{1,k}(x_1) dx_1 \ , \tag{23}$$

where $f_{0,k,max}(x)$ is the PDF of the maximum correlation coefficient of the inactive group at iteration k and $f_{1,k}(x)$ is the PDF of the k-th greatest correlation coefficient of the active group, i.e. the coefficient that must be selected at iteration k for a successful detection.

Concerning the signal estimation, the algorithm's performance is analyzed through the average SER. The SER approximation is obtained by studying the SNR of the considered symbol. This SNR is denoted by ρ_0 as stated before, but affected by a coefficient G which derives from the elements of the matrix signature $B^{(n)}$. This coefficient is defined as a Chi-squared distributed random variable, leading to its PDF

$f_G(x)$. Assuming that a QPSK modulation have been used, the average SER is then derived :

$$SER \approx \int_0^{+\infty} \left[erfc(\sqrt{0.5\rho_0 g}) - [0.5 erfc(\sqrt{0.5\rho_0 g})]^2 \right] f_G(g) dg \tag{24}$$

The validation of the actual improvement is based on simulation results, to which the theoretical approximated SER and Group User Detection Success Rate are also confronted. Different cases with varying numbers of users, active users, antennas, maximum algorithm iterations, transmission probabilities and/or SNRs are simulated with either the BOMP, normalized BOMP or ICBOMP to compare their performances in term of Group User Success Rate and SER. The computational cost of the algorithms is also depicted in the simulations results. The figures 10, 11,12 are some of the results of the simulations, evaluating the individual User Detection Success Rate (UDSR), Group User Detection Success Rate (GUDSR) and SER performance of BOMP, N-BOMP (numerically and from the theoretical expression) and ICBOMP:

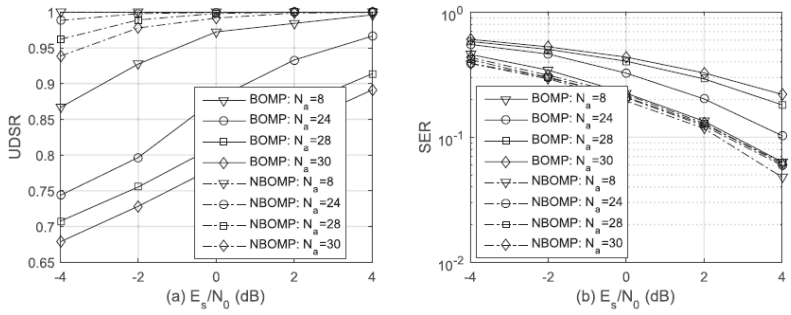

Figure 10: BOMP and N-BOMP performance for $\alpha = 8$ antennas, $N = 80$ nodes, $N_{a\ max} = 30$ iterations, the data size $d = 100$ symbols and the message length $m = 500$ symbols.[30]

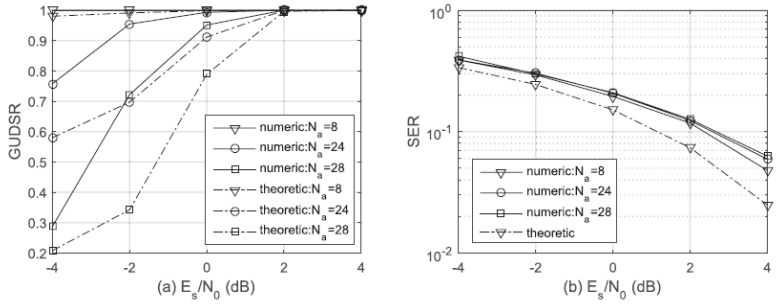

Figure 11: N-BOMP numerical and theoretical performances for $\alpha = 8$ antennas, $N = 80$ nodes, $N_{a\ max} = 30$ iterations, the data size $d = 100$ symbols and the message length $m = 500$ symbols.[30]

The paper shows a more accurate recovery of small packets by using precoding, error detection and correction codes, and ICBOMP scheme while this proposition

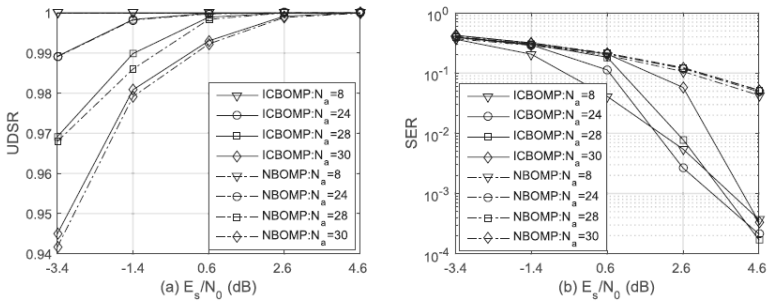

Figure 12: N-BOMP and ICBOMP performances for $\alpha = 8$ antennas, $N = 80$ nodes, $N_{a\ max} = 30$ iterations, the data size $d = 124$ symbols and the message length $m = 620$ symbols.[30]

also requests less computational resources. The ICBOMP outperforms both BOMP and N-BOMP. The simulations also comfort the theoretical expressions of N-BOMP performances, which is an improvement of the BOMP algorithm.

5.4 Remarks and Perspectives

To go further in the design of a Medium Access technique fully dedicated to massive IoT under URLL and LPWA constraints, some modifications can be brought to the model discussed in section 5.3.1.

For example, in order to improve the reliability, a Maximum A Posteriori estimator, which would use the different activity rates of the users, can be integrated to the decoder, but at the cost of a complexity increase at the receiver.

Moreover, it is important to consider the synchronization feasibility of this MAC, closely linked to the physical layer, to enlighten the impact (and so the cost) of synchronization on the latency, the resources and the energy consumptions in comparison with the reliability of the communications. This study would also show how close it is possible to approach the ideal asynchronous framework in order to allow "one-shot" transmissions scheme. Similarly, a strong assumption for the application of this model is the perfect channels knowledge, requiring a large amount of temporal/ frequency/ energy resources, which is not so realistic for a massive IoT network. The same trade-offs between reliability and efficiency can thus be observed for this requirement.

In the description of the model as used up to now, the channel responses only comprise fading effect. In real conditions, a path loss should also be considered. The model can nevertheless stand with a path loss gain hypothesis, if the messages are considered to be sent at a power level that compensates the path loss. In that case, a power control is employed: taking advantage of some potential broadcast beacons needed in the synchronization part for allowing the nodes to estimate their path loss gains before transmitting, the nodes are then able to send their messages at a power level depending on their previous estimation. All nodes messages are thus received at approximately the same power level, which corresponds to the equation 21.

However, this power control places cell edge nodes in an unfavorable condition for their lifetime. Indeed, these nodes will consume more power than a node closer to the Cellular Base Station, causing a reduction of its expected lifetime. This is

a critical issue since IoT LPWA devices are assumed to be power efficient for lasting dozens of years without requiring any intervention. Furthermore, receiving at the same power might have a negative impact on the detection since in the proposed approach the receiver exploits a SIC technique, which relies on power level difference between superposed signals. Therefore, a solution for optimizing the power control balanced with reliability must be investigated.

6 Conclusion

The emergence of new IoT applications such as NB-IoT requires to fulfill and meet several challenges. This report covers several aspects of IoT such as the power consumption, the coverage, the allocated bandwidth, the reliability and the latency. Reducing the energy consumption is one of the major features of NB-IoT end devices. This target is inherently correlated to enhancing the coverage and to optimizing the allocated bandwidth. Currently, the fundamental adopted solution in NB-IoT is to increase the number of retransmissions, and thereby consuming more energy. In the first part of this report, we established a tradeoff between the density of nodes and the allocated bandwidth required to handle the overall trafic in the network. We have also shown the impact of SIMO transmission in improving this tradeoff. In the second part, we have proposed a new solution based on dynamic spectrum using machine learning algorithms in order to enhance the coverage and to reduce the energy consumption. The random selection procedure is replaced by a more efficient selection method that chooses the channels with the highest probability to be available, and with the best coverage and the lowest number of required repetitions. Finally, the third part of the report proposes a Compressive Sensing model for the MAC layer design of Ultra Reliable Low Latency network with low power constraint.

A A primer on spatial Poisson Point Process

A.1 Spatial Poisson Point Process

Definition 1 (Spatial PPP and Marked PPP). *A random distribution of points Φ is called an homogeneous PPP of intensity λ if:*

- *The number of points of Φ in any set $\mathcal{S}$, $|\Phi(\mathcal{S})|$, is a Poisson random variable with mean λ times the surface of $\mathcal{S}$.*
- *The numbers of points $\Phi(\mathcal{S}_i)$ of Φ in disjoint sets $\mathcal{S}_i$ are independent random variables.*

An independent Marked Poisson Point Process is the collection of pairs $\tilde{\Phi} = \{(x_i, m_i)\}_i$, where $\{x_i\}$ is the set of points and $\{m_i\}$ the set of independent marks.

A.2 Properties of PPPs

1. Superposition of independent PPPs with intensities λ_k is a PPP and its intensity is $\sum_k \lambda_k$;
2. Independent Thinning of a PPP with a constant factor p is a PPP and its intensity is $p\lambda$;
3. By Slivnyak's theorem, adding a singleton to a PPP preserves the PPP;

A.3 Useful Theorems

Theorem 1 (Campbell Theorem, [5]). *Let $f : \Phi \to \mathbb{R}$ a measurable function where Φ is a PPP on $\mathbb{R}^2$ with intensity λ,*

$$\mathbb{E}\left[\sum_{x\in\Phi} f(x)\right] = \lambda \int_{\mathbb{R}^2} f(x)dx.$$

Theorem 2 (Benett's Concentration Inequality, [33]). *Let X_i a bounded independent random variable $X_i < a$, $X = \sum_{i=1}^{N} X_i$ with average m_x and $v_x = \sum_{i=1}^{N} \mathbb{E}(X_i^2)$,*

$$Prob\{X > \alpha m_x\} \leq \exp\left(-\frac{v_x}{a^2} g\left(\frac{(\alpha-1)m_x a}{v_x}\right)\right),$$

for $\alpha \geq 1$ and $g(t) = (1+t)\log(1+t) - t$.

B First and second moment expression

In order to compute the upper-bound on the outage probability, the first and the second moment on $N_{RR,t}(o)$ should be computed. We can first notice that $\Phi_c(o)$ is not an homogeneous PPP. Assuming a node x situated at a distance r from o, this

node belongs to $\Phi_c(o)$ if the ball around this node does not contain any collector with probability $e^{-\lambda_b \pi r^2}$. This means that,

$$m_N = \mathbb{E}\Big[\sum_{x\in\Phi_c(o)} N_{RR}(x)\Big] = \mathbb{E}_{\Phi,\Phi_b,A_f,I}\Big[\sum_{x\in\Phi} \underbrace{\prod_{y\in\Phi_b} N_{RR}(x)\ \mathbb{1}_{\{|x|<|y-x|)\}}}_{f(x)}\Big]$$

Using Campbell Theorem,

$$m_N = \lambda_a \int \mathbb{E}_{\Phi_b}\big[f(x)\big]dx.$$

with $dx = rdrd\theta$ and

$$\mathbb{E}_{\Phi_b}\big[f(x)\big] = N_{RR}(x)\ \mathbb{E}_{\Phi_b}\Big[\prod_{y\in\Phi_b} \mathbb{1}_{\{|x|<|y-x|)\}}\Big] = N_{RR}(x)\exp(-\lambda_b\pi r^2).$$

Using the PGFL,

$$\prod_{y\in\Phi_b} \mathbb{1}_{\{|x|<|y-x|)\}} = \exp\Big(-\lambda_b \int (1-\mathbb{1}_{\{|x|<|y-x|)\}})dy\Big),$$

with

$$\int (1-\mathbb{1}_{\{|x|<|y-x|)\}})dy = \int (1-\mathbb{1}_{\{|y-x|>r)\}})dy = \int (1-\mathbb{1}_{\{|z|>r)\}})dz = \pi r^2.$$

Thus,

$$m_N = \frac{\lambda_a}{\lambda_b}\ \mathbb{E}_I\left[\int\int N_{RR}(r,A_f,I)\ 2\pi\lambda_b r\exp(-\lambda_b\pi r^2)\ p(A_f)dr\ dA_f\right].$$

Notice that

$$p(r) = 2\pi\lambda_b r\exp(-\lambda_b\pi r^2),$$

is nothing but the pdf of the smallest distance between the sensor and its nearest collector. This implies that,

$$m_N = \frac{\lambda_a}{\lambda_b}\ \mathbb{E}_r\ \mathbb{E}_I\ \mathbb{E}_{A_f}[N_{RR}(r,A_f,I)].$$

References

[1] G. T. . v13.1.0, "Cellular system support for ultra low complexity and low throughput internet of things," *[Online]*, November 2015.

[2] N. Sornin, M. Luis, T. Eirich, T. Kramp, and O. Hersent, "LoRa Alliance LoRaWAN specification," *LoRaWAN Specifiction, Release v1. 0*, 2015.

[3] M. Anteur, V. Deslandes, N. Thomas, and A.-L. Beylot, "Ultra narrow band technique for low power wide area communications," in *Global Communications Conference (GLOBECOM), 2015 IEEE*. IEEE, 2015, pp. 1–6.

[4] J. G. Andrews, A. K. Gupta, and H. S. Dhillon, "A primer on cellular network analysis using stochastic geometry," *CoRR*, vol. abs/1604.03183, 2016. [Online]. Available: http://arxiv.org/abs/1604.03183

[5] F. Baccelli and B. Blaszczyszyn, "Stochastic Geometry and Wireless Networks: Volume I Theory," *Foundations and Trends in Networking*, vol. 3, no. 34, pp. 249–449, 2010.

[6] ——, "Stochastic Geometry and Wireless Networks: Volume II Application," *Foundations and Trends in Networking*, vol. 4, no. 12, pp. 1–312, 2010.

[7] M. Haenggi and R. Ganti, "Interference in Large Wireless Networks," *Foundations and Trends in Networking*, vol. 3, no. 2, pp. 127–248, 2009.

[8] R. Giacomelli, R. Ganti, and M. Haenggi, "Outage Probability of General Ad Hoc Networks in the High-Reliability Regime," *IEEE/ACM Transactions in Networking*, vol. 19, no. 4, pp. 1151–1163, 2011.

[9] M. Haenggi, "Outage, local throughput, and capacity of random wireless networks," *IEEE Transactions on Wireless Communications*, vol. 8, no. 8, pp. 4350–4359, 2009.

[10] S. Weber, J. G. Andrews, and N. Jindal, "An overview of the transmission capacity of wireless networks," *IEEE Trans. On Communications*, vol. 56, no. 12, pp. 3593–3604, 2010.

[11] S. Weber, X. Yang, J. G. Andrews, and G. de Veciana, "Transmission Capacity of Wireless Ad Hoc Networks with Outage Constraints," *IEEE Trans. on Information Theory*, vol. 51, no. 12, pp. 4091–4102, 2005.

[12] L. Decreusefond, E. Ferraz, and P. Martins, "Upper Bound of Loss probability for the dimensioning of OFDMA systems with multi class randomly located users," in *WiOpt, workshop SPASWIN, IEEE 2009*. IEEE, 2009.

[13] L. Decreusefond, E. Ferraz, P. Martins, and T. T. Vu, "Robust methods for LTE and WiMAX dimensioning," in *6th International Conference on Performance Evaluation Methodologies and Tools*. IEEE, 2012.

[14] F. Kaddour, P. Martins, L. Decreusefond, E. Vivier, and L. Mroueh, "Robust methods for LTE and WiMAX dimensioning," in *6th International Conference on Performance Evaluation Methodologies and Tools*. IEEE, 2013.

[15] L. Mroueh, A. Kessab, P. Martins, S. Hethuin, and E. Vivier, "Radio Resource Dimensioning in a Centralized Ad-Hoc Maritime MIMO LTE Network," in *IEEE Sarnoff conference*. IEEE, 2013.

[16] F. Dehmas, C. Bader, D. Duchemin, L. Mroueh, and G. Vivier, "Scenarios and requirements," *EPHYL project delivrable 2.1*, 2017.

[17] "Coverage analysis of LTE-M category M1," *White Paper*, 2017.

[18] W. Jouini, D. Ernst, C. Moy, and J. Palicot, "Upper confidence bound based decision making strategies and dynamic spectrum access," in *2010 IEEE International Conference on Communications*, May 2010, pp. 1–5.

[19] L. Melian-Gutierrez, N. Modi, C. Moy, I. Perez-Alvarez, F. Bader, and S. Zazo, "Upper Confidence Bound learning approach for real HF measurements," in *2015 IEEE International Conference on Communication Workshop (ICCW)*, June 2015, pp. 381–386.

[20] P. Auer, "Using confidence bounds for exploitation-exploration trade-offs," *Journal of Machine Learning Research*, vol. 3, no. Nov, pp. 397–422, 2002.

[21] V. e. a. Saxena, "Reducing the Modem Complexity and Achieving Deep Coverage in LTE for Machine-Type Communications," in *Global Communications Conference (GLOBECOM), 2016 IEEE*. IEEE, 2016, pp. 1–7.

[22] W. Jouini, C. Moy, and J. Palicot, "Decision making for cognitive radio equipment: analysis of the first 10 years of exploration," *Eurasip journal on wireless communications and networking*, vol. 2012, no. 1, p. 26, 2012.

[23] R. Bonnefoi, C. Moy, and J. Palicot, "LPWAN AMI Bachaul Latency- Improvement with Reinforcement Learning Algorithms."

[24] R. Rapeepat, B. Vejlgaard, N. Mangalvedhe, and A. Ghosh, "NB-IoT system for M2M communication," in *Wireless Communications and Networking Conference (WCNC), 2016 IEEE*. IEEE, 2016, pp. 1–5.

[25] A. K. Fletcher, S. Rangan, and V. K. Goyal, "Necessary and Sufficient Conditions for Sparsity Pattern Recovery," *IEEE Transactions on Information Theory*, vol. 55, no. 12, pp. 5758–5772, dec 2009. [Online]. Available: http://ieeexplore.ieee.org/document/5319742/

[26] ——, "On-Off Random Access Channels: A Compressed Sensing Framework," mar 2009. [Online]. Available: http://arxiv.org/abs/0903.1022

[27] Y. Ji, C. Stefanovic, C. Bockelmann, A. Dekorsy, and P. Popovski, "Characterization of coded random access with compressive sensing based multi-user detection," in *2014 IEEE Global Communications Conference*.

IEEE, dec 2014, pp. 1740–1745. [Online]. Available: http://ieeexplore.ieee.org/document/7037060/

[28] J. Scarlett and V. Cevher, "Limits on support recovery with probabilistic models: An information-theoretic framework," in *2015 IEEE International Symposium on Information Theory (ISIT)*. IEEE, jun 2015, pp. 2331–2335. [Online]. Available: http://ieeexplore.ieee.org/document/7282872/

[29] C. Rush, A. Greig, and R. Venkataramanan, "Capacity-Achieving Sparse Superposition Codes via Approximate Message Passing Decoding," *IEEE Transactions on Information Theory*, vol. 63, no. 3, pp. 1476–1500, mar 2017. [Online]. Available: http://ieeexplore.ieee.org/document/7809025/

[30] R. Xie, H. Yin, X. Chen, and Z. Wang, "Many Access for Small Packets Based on Precoding and Sparsity-Aware Recovery," *IEEE Transactions on Communications*, vol. 64, no. 11, pp. 4680–4694, nov 2016. [Online]. Available: http://ieeexplore.ieee.org/document/7558184/

[31] H. Nikopour and H. Baligh, "Sparse code multiple access," in *IEEE International Symposium on Personal, Indoor and Mobile Radio Communications, PIMRC*, 2013.

[32] G. Wunder, C. Stefanovic, P. Popovski, and L. Thiele, "Compressive coded random access for massive MTC traffic in 5G systems," in *2015 49th Asilomar Conference on Signals, Systems and Computers*. IEEE, nov 2015, pp. 13–17. [Online]. Available: http://ieeexplore.ieee.org/document/7421050/

[33] S. Weber, X. Yang, J. G. Andrews, and G. de Veciana, "Probability inequalities for the sum of independent random variables," *Journal of the American Statistical Association*, 1962.